Earliest Silurian graptolites from Kalpin, western Tarim, Xinjiang, China

Wenhui Wang, Lucy A. Muir, Xu Chen & Peng Tang

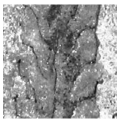

A graptolite fauna containing 13 species in seven genera is described from the basal part of the Middle Member of the Kalpintag Formation, in the Kalpin region of Xinjiang Province, northwestern China. The taxa are *Avitograptus* sp. aff. *A. avitus* (Davies), *Hirsutograptus jideliensis* (Koren' & Mikhailova), *Korenograptus laciniosus* (Churkin & Carter), *K. jerini* (Koren' & Melchin), *K.* aff. *K. magnus* (Churkin & Carter), *Metabolograptus wangjiawanensis* (Mu & Lin), *M. parvulus* (Lapworth), *Normalograptus ajjeri* (Legrand), *N. angustus* (Perner), *N. mirnyensis* (Obut & Sobolevskaya), *Paramplexograptus madernii* (Koren' & Mikhailova), *Par.*? sp., and *Persculptograptus* sp. Approximately half of the species described have not been previously recorded from the Kalpin region. An early Silurian (Rhuddanian) age is indicated by *H. jideliensis* and *K. jerini.* The graptolite fauna recovered from the four sections in the Kalpin region shares numerous common species with faunas from the Yangtze region of China and from southern Kazakhstan. • Key words: Graptoloidea, earliest Silurian, Xinjiang Province, China.

Wang, W., Muir, L.A., Chen, X. & Tang, P. 2015. Earliest Silurian graptolites from Kalpin, western Tarim, Xinjiang, China. *Bulletin of Geosciences 90(3)*, 519–542 (8 figures, 2 tables). Czech Geological Survey, Prague. ISSN 1214-1119. Manuscript received December 8, 2014; accepted in revised form March 29, 2015; published online May 12, 2015; issued September 30, 2015.

Wenhui Wang (corresponding author), School of Earth Sciences and Engineering, Nanjing University, 163 Xianlin Street, 210023 Nanjing, China; wwhever@126.com • Wenhui Wang & Xu Chen, Key Laboratory of Economic Stratigraphy and Palaeogeography, Nanjing Institute of Geology and Palaeontology, 39 East Beijing Road, 210008 Nanjing, China • Lucy A. Muir, Chatsworth, Spa Road, Llandrindod Wells, Powys, LD1 5EY, UK • Peng Tang, State Key Laboratory of Palaeobiology and Stratigraphy, Nanjing Institute of Geology and Palaeontology, 39 East Beijing Road, 210008 Nanjing, China

The latest Ordovician to earliest Silurian interval, during which significant geological and biological events occurred, was the focus of much research attention during the later part of the last century (*e.g.* Melott & Thomas 2009, Harper *et al*. 2013, Baarli 2014). Because of their use in biostratigraphy, graptolites from strata near the Ordovician–Silurian boundary have been well studied from many localities worldwide. In China, particularly in South China, much research effort was put towards determining the precise location of the Ordovician–Silurian boundary and defining the graptolite biostratigraphy, resulting in the recognition of regional graptolite biozones and allowing global biostratigraphical correlation (Chen *et al*. 2000a, 2005; Fan *et al*. 2011). Moreover, studies of graptolite diversity from South China have clearly revealed the stepwise pattern of the Late Ordovician–early Silurian extinction-recovery event (Fan & Chen 2007). More recently, Ordovician and Silurian graptolite biostratigraphy and geography have been used to analyze the temporal and spatial distributions of black shales, which are the main shale gas source beds in South China (Fan *et al*. 2011).

In regions outside South China, such as the Tarim region of western China, due to difficulty in gaining access to the area, graptolites from the Ordovician–Silurian boundary have rarely been collected and are not yet well understood. Studies of graptolites from the Kalpin area in the Tarim region of western Xinjiang were first conducted in the 1960s (*e.g*., Mu *et al*. 1960). Since then, detailed systematic and stratigraphic studies have been carried out (Chen *et al*. 2000b), resulting in the Dawangou section near Kalpin being confirmed as a global auxiliary stratotype section of the Upper Ordovician (Chen & Wang 2003). Most of these studies focused on graptolites from the Upper Ordovician Qilang and Yingan formations, while little attention has been paid to graptolites from the Kalpintag Formation, in which the Ordovician–Silurian boundary was thought to be located. In the Kalpin area, graptolites including *Climacograptus alternis* Packham, 1962, *Glyptograptus elegans* Packham, 1962, *G. incertus* Elles & Wood, 1907, *G. tamariscus* (Nicholson, 1868), *G. tangshanensis* (Hsü, 1934), and *G. sinuatus* (Nicholson, 1869) were recorded by Zhou *et al.* (1991). This species association

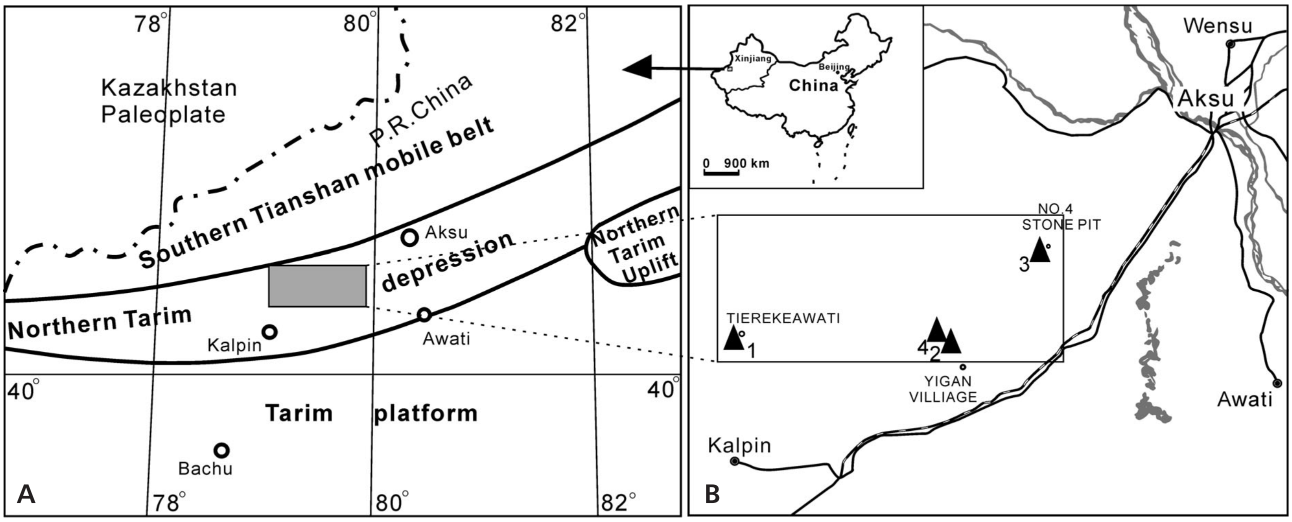

Figure 1. A – geological setting of the Kalpin region, modified after Feng *et al*. (2007) and Chen *et al*. (2000). • B – locality map of the Kalpin region, Northern Tarim depression, northwest China. Section numbers represent: 1 – Tierekeawati section; 2 – Dawangou East section; 3 – Sishichang section; 4 – Dawangou section. The approximate location of the four sections depicted in box in Fig. 1A is indicated by the box northeast of Kalpin in Fig. 1B.

indicated an early Silurian age. Subsequently, graptolites were recorded from bore cores in the Kalpintag Formation by Zhan (1996, 1997), which greatly improved the knowledge of early Silurian graptolites from this region. No systematic stratigraphic work was carried out until 1997, when Ni & Chen (1997) reported graptolites from boreholes in the northern Tarim Basin. The horizon that yielded species including *Glyptograptus elegans*, *G. incertus*, *G. enodus* Packham, 1962 and *Normalograptus tangshanensis linearis* (Packham, 1962) was considered to be equivalent to the Middle Member of the Kalpintag Formation. The most recent graptolite research in this area was carried out by Jiang *et al*. (2006). They undertook continuous collecting of graptolites in the basal part of the Middle Member of the Kalpintag Formation. Recovery of *Normalograptus*, *Paraclimacograptus*, *Rhaphidograptus* and *Rivagraptus* indicated that the basal part of the Middle Member of the Kalpintag Formation is probably latest Rhuddanian to earliest Aeronian in age. Thus, Jiang *et al*. (2006) tentatively suggested that the Ordovician–Silurian boundary lies in the basal part of the Middle Member or in the upper part of the Lower Member of the Kalpintag Formation. However, because no systematic illustrations and descriptions were provided in their study, and no important and characteristic graptolite taxa that can definitely establish the age were recovered, the association of early Silurian graptolites from this bed is still not well understood.

By checking the specimens collected by Jiang *et al*. (2006), together with new collections from the basal part of the Middle Member of the Kalpintag Formation in three other sections in the Kalpin area, this study revises some of the taxonomic assessments of Jiang *et al*. (2006), but confirms the presence of *Korenograptus laciniosus* (Churkin & Carter, 1970). In new collections made in 2012, characteristic early Silurian (Ruddanian) species including *Korenograptus jerini* (Koren' & Melchin, 2000) and *Hirsutograptus jideliensis* (Koren' & Mikhaylova *in* Koren' *et al*., 1980) were found. The aim of this study is to provide a detailed systematic and biostratigraphic study of these earliest Silurian graptolites from the Kalpin region, Tarim area. In addition, we provide important biostratigraphical evidence that will help to locate the position of the Ordovician–Silurian boundary in this area of northwestern China.

Geological setting and material

From southeast to northwest, four tectonic units form the Northwestern Tarim palaeoplate: the Tarim platform, the northern Tarim depression, the northern Tarim uplift, and the southern Tian Shan mobile belt (Chen *et al*. 1995, Feng *et al*. 2007; Fig. 1A). The Kalpin region is located at the northern edge of the northern Tarim depression, on the southwestern flank of the Tian Shan mountain range (Fig. 1A).

All of the specimens from the four sections were collected from the basal part of the Middle Member of the Kalpintag Formation. The interval is characterized by thin- and medium-bedded, greyish-green, arenaceous mudstones with an overall thickness of 0.5–1.5 m. The Middle Member of the Kalpintag Formation in the Kalpin area is 60–160 m thick (Fig. 2).

The specimens described herein were collected on two separate occasions. The major portion of the material was

Table 1. Distribution of graptolite species in the four studied sections in the Middle Member of the Kalpintag Formation in the Tarim region. Note: * present; – absent. XKDE section: Dawangou East section; XAS section: Sishichang section; XAT section: Tierekeawati section; XKD: Dawangou section.

Species	XKDE section	XAS section	XKD section	XAT section
Avitograptus sp. aff. *A. avitus* (Davies, 1929)	*	–	*	–
Hirsutograptus jideliensis (Koren' & Mikhailova *in* Koren' *et al*., 1980)	–	–	*	*
Korenograptus laciniosus (Churkin & Carter, 1970)	*	–	*	–
Korenograptus aff. *K. magnus* (Churkin & Carter, 1970)	–	*	–	–
Korenograptus jerini (Koren' & Melchin, 2000)	*	*	–	*
Metabolograptus wangjiawanensis (Mu & Lin, 1984)	*	*	–	–
Metabolograptus parvulus (Lapworth, 1900)	*	–	*	*
Normalograptus ajjeri (Legrand, 1977)	*	–	–	*
Normalograptus angustus (Perner, 1895)	–	–	–	*
Normalograptus mirnyensis (Obut & Sobolevskaya *in* Obut *et al*., 1967)	–	*	*	*
Paramplexograptus madernii (Koren' & Mikhailova *in* Koren' *et al*., 1980)	*	–	*	–
Paramplexograptus? sp.	*	*	–	*
Persculptograptus sp.	*	*	–	*

collected during September 2012 from three localities in Xinjiang Province, northwest China: the Tierekeawati section, near the village of the same name in the Kalpin area (GPS co-ordinates N 40° 43´ 10.85˝, E 79° 03´ 54.42˝); the Dawangou East section, near Yingan village, Aksu area (GPS co-ordinates N 40° 42´ 41.4˝, E 79° 33´ 64.2˝); and the Sishichang section in the Aksu area (GPS co-ordinates N 40° 50´ 17.6˝, E 79° 50´ 09.4˝). A small number of specimens were collected and reported on by Jiang *et al*. (2006). These were from the Middle Member of the Kalpintag Formation in the well-known Dawangou section (GPS coordinates N 40° 42´ 46.65˝, E 79° 32´ 29.71˝) (Fig. 1B). Other fossils recorded from these sections are brachiopods, acritarchs, chitinozoans, fish, and conulariids (Zhou 2001).

Results

Although a considerable portion of the graptolites are broken or poorly preserved, most are moderately to well preserved in partial to full relief. The occurrences of species in each section are listed in Table 1.

In contrast to the normalograpid (N) fauna, which is characterized by high specific and low generic diversity during the late Hirnantian in the Yangtze region, South China, the graptolite fauna described herein contains 13 graptolite species attributed to seven genera (Table 1). The abundance of each species differs greatly; some species, *e.g. Korenograptus laciniosus*, *Hirsutograptus jideliensis*, *Normalograptus ajjeri*, *N. mirnyensis*, *Persculptograptus* sp., and *Metabolograptus parvulus*, are numerically abundant, while others, *e.g. Korenograptus jerini* and *Normalograptus angustus*, have low abundance.

Discussion

The precise position of the Ordovician–Silurian boundary remains unknown in the northern Tarim region due to the lack of correlatable faunas from the *Persculptograptus persculptus* and *Akidograptus ascensus–Parakidograptus acuminatus* biozones. Before the 1990s, the Yingan Formation was regarded as being of latest Ordovician age, and was suggested to have a disconformable contact with the overlying Kalpintag Formation. A small hiatus could be present between the Yingan and Kalpintag formations. The latter was thought to be Silurian in age (Zhou *et al*. 1991). The Kalpintag Formation can be divided into Lower, Middle, and Upper members. Based on evidence from graptolites, trilobites, and chitinozoans, Zhou (2001) proposed that the Kalpintag Formation has an age range of "Ashgill" (Late Ordovician) to Aeronian (early Silurian), and the position of the Ordovician–Silurian boundary in the northern Tarim region may be between the Lower and Middle members of the Kalpintag Formation. Geochemical studies conducted on the argillaceous carbonate rocks in the basal part of the Middle Member of the Kalpintag Formation showed abnormal geochemical patterns, including those for CaO, Sr, Ce/La, Ni, and Cu. Combined with biostratigraphical evidence, Jiang *et al*. (2001) proposed that the O–S boundary is located in the argillaceous carbonate rocks. However, their fossil evidence was somewhat weak due to poor preservation. Based on graptolite records, Jiang *et al*. (2006) proposed that the basal part of the Middle Member of the Kalpintag Formation is probably latest Rhuddanian to earliest Aeronian in age. However, in the present study, graptolite species such as *Korenograptus jerini* and *Hirsutograptus jideliensis* were identified from nearby sections, indicating

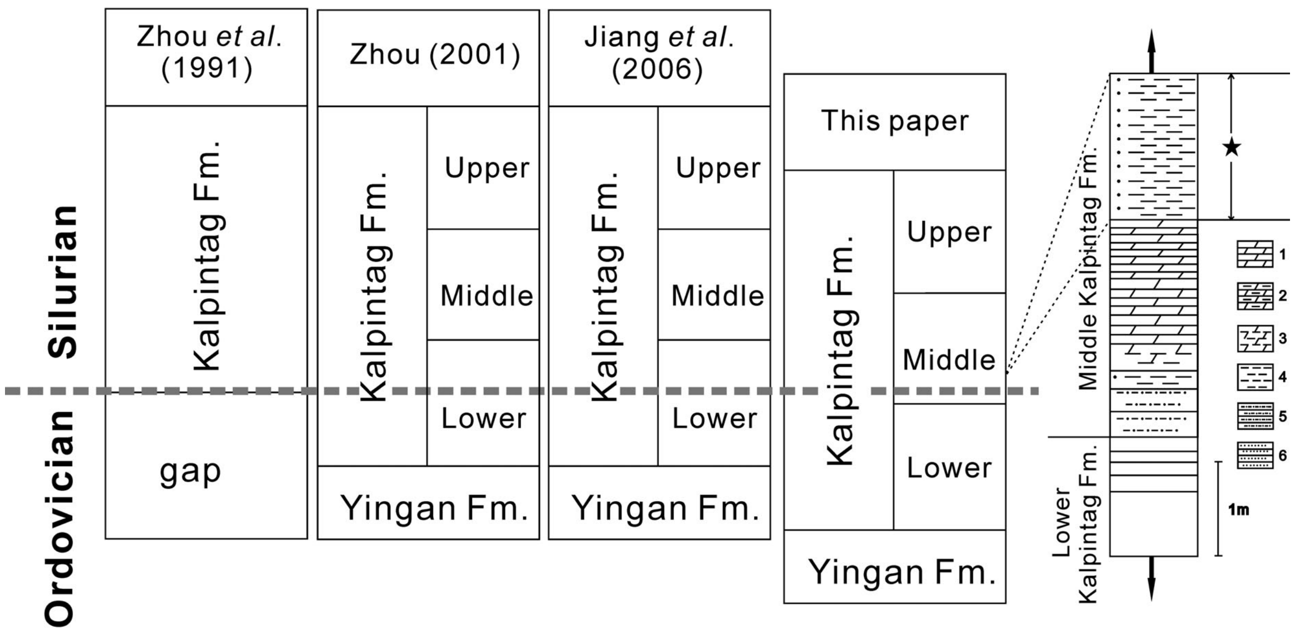

Figure 2. The position of the Ordovician–Silurian boundary (dotted line) in the northern Tarim region in previous literature and this study. The stratigraphical column was measured in the Dawangou section by Jiang *et al*. (2006). The stratigraphical columns of the other three sections are similar to that of the Dawangou section, and differ only in the thickness of each rock type. Symbols represent: 1 – argillaceous dolomite; 2 – lime-dolomite; 3 – dolomitic mudstone; 4 – mudstone; 5 – siltstone; 6 – sandstone. The star indicates the graptolite-bearing beds.

a probably different, earlier age for the basal part of the Middle Member of the Kalpintag Formation.

The graptolite fauna described herein contains several species, and can be divided into two groups. One group consists of species that have only been reported from lower Silurian rocks and have a short stratigraphical range; the second group contains species that have been reported from late Ordovician to lower Silurian strata.

The first group contains *Hirsutograptus jideliensis* and *Korenograptus jerini* (originally "*Glyptograptus jerini*" Koren' & Melchin, 2000). *Hirsutograptus jideliensis* was first reported from the *Pk. acuminatus* Biozone of Kazakhstan (Koren' & Mikhailova *in* Koren' *et al*., 1980). Later the species was collected from the Kurama Ridge in eastern Uzbekistan, in the *Normalograptus lubricus*, *Akidograptus cuneatus*, and *Hirsutograptus sinitzini* subzones of the *Ak. ascensus–Pk. acuminatus* Biozone) (Koren' & Melchin 2000). *Korenograptus jerini* was first reported from the *Ak. cuneatus* and *H. sinitzini* subzones (*Ak. ascensus–Pk. acuminatus* Biozone) of the Kurama Ridge, eastern Uzbekistan (Koren' & Melchin 2000).

The second group, of longer-ranging species, includes *Avitograptus* sp. aff. *A. avitus* (Davies, 1929), *Normalograptus ajjeri*, *N. angustus*, *N. mirnyensis*, *Metabolograptus wangjiawanensis*, *M. parvulus*, and *Paramplexograptus madernii*. Loydell (2007) suggested that many previous records of *N. normalis* could be considered to be *N. ajjeri*. Thus, *N. ajjeri* clearly has a long stratigraphical range, from the Hirnantian to the lower Aeronian (Loydell 2007). *Normalograptus angustus* has an even longer stratigraphical range, from the *Pleurograptus linearis* Biozone (Skoglund 1963), through the Hirnantian (Chen *et al*. 2005) and into the *Coronograptus cyphus* Biozone of the Rhuddanian (Rickards 1970, Hutt 1974). *Normalograptus mirnyensis* ranges from the *M. extraordinarius* Biozone through to the *P. persculptus* Biozone in South China (Chen *et al*. 2005). In eastern Uzbekistan, the species is found in the *N. lubricus*, *A. cuneatus*, and *H. sinitzini* subzones (*Ak. ascensus–Pk. acuminatus* Biozone; Koren' & Melchin 2000). The range of *Metabolograptus wangjiawanensis* extends from the *P. persculptus* Biozone through to the lower part of the *Akidograptus ascensus* Biozone in South China (Chen *et al*. 2005). In Arctic Canada, this species has been recorded from the *P. persculptus* Biozone (Melchin *et al*. 1991). *Paramplexograptus madernii* was first reported in Kazakhstan from the *Pk. acuminatus* Biozone (Koren' & Mikhailova *in* Koren' *et al*., 1980), and was recently reported in the *Pk. acuminatus* Biozone? of Cape Manning, Nunavut, Canada (Melchin & Holmden 2006, Melchin *et al*. 2011). "*Normalograptus* sp. aff. *N. indivisus* (Davies, 1929)", identified by Chen *et al*. (2005), is regarded as *Paramplexograptus madernii* in this study; thus, the range of this species now extends to the Ordovician *P. persculptus* Biozone. *Avitograptus avitus* was reported from the *P. persculptus* to the *Pk. acuminatus* biozones in Scotland, Scandinavia, and South China (Davies 1929, Williams 1983, Chen *et al*. 2005, Maletz *et al*. 2014); in southwestern Sweden it ranges through the *A. avitus* s.s. fauna, with a post-*P. persculptus* and pre-*A. ascensus* age (Koren' *et al*. 2003, Maletz *et al*. 2014). *Metabolograptus parvulus* is confined to the Ordovician *P. persculptus* Biozone and the lower part of the Silurian *Pk. acuminatus* Biozone in Great Britain (Williams 1983, Zalasiewicz & Tunnicliff 1994). In Arctic Canada and South China, it has been recorded only from the upper part of the *P. persculptus* Biozone (Melchin *et al*. 1991, Chen *et al*. 2005). In Jordan, this species ranges through to the top of the *Ak. ascensus–Pk. acuminatus* Biozone and possibly into the succeeding *Cystograptus vesiculosus* Biozone (Loydell 2007). Thus, its overall range appears to be *P. persculptus* to at least upper *Ak. ascensus–Pk. acuminatus* biozones.

The graptolite assemblages described herein lacks akidograptids, thus making it difficult to recognize the lower boundary of the Silurian. Such an assemblage by no means unique, *e.g*. in Arctic Canada, the Algerian Sahara, South Kazakhstan, and the Kurama Range of Uzbekistan, a lowermost Ruddanian diplograptid fauna lacking akidograptids is frequently observed (Melchin 1998, Koren' & Melchin 2000). Koren' *et al*. (2003) called these assemblages the "post-*persculptus* diplograptid fauna". Environmental conditions are suggested to be responsible for the absence of akidograptids in these graptolite associations. Despite the lack of akidograptids that can be used to identify the base of the Silurian definitively, the present graptolite fauna contains species that are certainly of earliest Silurian age, and has no species that occur only in uppermost Ordovician strata, indicating that the basal part of the Middle Member of the Kalpintag Formation in the Kalpin region is most likely to be Rhuddanian in age (from the *Ak. ascensus* Biozone to the *Pk. acuminatus* Biozone). Our graptolite results indicate that the Ordovician–Silurian boundary is situated below the graptolite-bearing beds.

Fossils found in the studied sections together with the graptolites are brachiopods, acritarchs, chitinozoans, fish, and conulariids (Zhou 2001). The similarities of the palynomorphs and fish from Tarim to those from the South China palaeoplate indicate that the two palaeoplates were quite close to each other and possibly located within the same palaeoclimaticl zone, the tropical zone near the palaeoequator (Fortey *et al*. 2003, Zhao *et al*. 2009, Wang 2010). Recent palaeomagnetic research also indicates that the Tarim palaeoplate, on the whole, showed a drift path from high northern to southern latitudes, and rapidly returned to northern latitudes during the Neoproterozoic to early Palaeozoic (Wang *et al*. 2013). During the latest Ordovician to Silurian interval, the Tarim basin was characterized by rapid deposition in a nearshore environment. This shallow-water environment is indicated by the presence of the *Eospirifer sinensis–Levenea* cf. *qianbeiensis* brachiopod assemblage in the Kalpintag Formation (Zhou 2001). In contrast to the South China paleoplate, which was in a deep-water environment and contained diverse graptolite taxa during the latest Ordovician to early Silurian, the shallow-water, rapid-deposition environment of the Tarim basin was not a favourable setting for graptolites after the Hirnantian extinction event. Thus, a relatively low-diversity graptolite fauna was recovered from this short interval. However, all of the reported species in the Tarim region are also known from South China. Therefore, the graptolite evidence is additional confirmation that the Tarim plate and South China may have been in the same palaeoclimatic zone.

Systematic palaeontology

Measurement of characters of graptolite rhabdosomes was carried out following Štorch *et al*. (2011, fig. 13). Astogenetic patterns (*e.g*., Patterns H and I) follow the descriptions of Mitchell (1987), Melchin & Mitchell (1991) and Melchin (1998). Open nomenclature and synonymy lists are based on Bengtson (1988) and Matthews (1973). All specimens are from the lowermost strata in the Middle Member of the Kalpintag Formation and are permanently deposited in the Laboratory of Palaeontology, Nanjing University.

Class Pterobranchia Lankester, 1877
Subclass Graptolithina Bronn, 1849
Infraclass Eugraptolithina Mitchell, Melchin, Cameron & Maletz, 2013
Division Graptoloida Lapworth, 1875,
emend. Mitchell, Melchin, Cameron & Maletz, 2013
Suborder Axonophora Frech, 1897
Infraorder Neograptina Štorch, Mitchell, Finney & Melchin, 2011

Superfamily Monograptoidea Lapworth, 1873, emend. Melchin *et al*., 2011
Paraphyletic family Dimorphograptidae Elles & Wood, 1908, emend. Melchin *et al*., 2011

Genus *Avitograptus* Melchin *et al*., 2011

Type species. – *Glyptograptus* (?) *avitus* Davies, 1929.

Diagnosis. – Species with Pattern J rhabdosomes, th1^1 upturned at level of sicular aperture, th1^2 arises from a point low within the upward-grown portion of th1^1, geniculate, slightly to moderately inclined thecae, slightly elongated first thecal pair relative to subsequent thecae, full median septum (Melchin *et al*. 2011).

***Avitograptus* sp. aff. *A. avitus* (Davies, 1929)**
Figures 3A, D, 7A

aff. *1929 *Glyptograptus*? *avitus* Davies, p. 8, fig. 21.
2005 *Normalograptus avitus* (Davies). – Chen *et al.*, p. 255, pl. 1, fig. 11; pl. 2, fig. 9; text-figs 7D, G, J–L.

Material. – Nine specimens: four from the Dawangou East section and five from the Dawangou section.

Description. – Rhabdosome up to 14 mm long, widening from 0.8–0.9 mm at the first thecal pair to the maximum width of 1.6–1.7 mm distally. The 2TRD is 1.55–1.9 mm at th2^1, 1.6 mm distally. The sicula bears a long and robust virgella that can reach a length of more than 5.5 mm. Thecae are glyptograptid in shape: the supragenicular walls are straight and slightly inclined to the rhabdosome axis, the genicula are rounded. Apertures are horizontal to slightly concave. Th1^1 is elongated, turns upward 0.15–0.2 mm below the sicular aperture and its upward-growing portion is 0.9–1.1 mm long. Th1^2 crosses the sicula diagonally, leaving the dorsal side of the sicula exposed for *ca* 0.4–0.55 mm. Median septum is complete.

Discussion. – Species included in *Avitograptus* are considered to have two important characters: first, elongation of the first thecal pair relative to the following thecae and, second, turning upward of the first theca at the sicular aperture. However, the second character is not an entirely consistent feature in the topotype collections, as suggested by Melchin *et al.* (2011). The present specimens are characterized by their elongate first two thecae, the large exposure of the antivirgellar wall under th1^2, and a long and robust virgella. Compared with the holotype of *A. avitus* illustrated by Williams (1983) and a mature topotype specimen illustrated by Melchin *et al.* (2011, fig. 6B) from the Dob's Linn section, the present specimens differ greatly in having a greater maximum width, larger apertural excavations, and by widening much more rapidly (Fig. 7A).

Stratigraphical range. – In South China, this taxon is known from the *P. persculptus* to the *Pk. acuminatus* biozones (Chen *et al.* 2005).

Superfamily Retiolitoidea Lapworth, 1873, emend. Melchin *et al.*, 2011
Paraphyletic family Neodiplograptidae Melchin *et al.*, 2011

Genus *Korenograptus* Melchin *et al.*, 2011

Type species. – *Glyptograptus gnomus* Churkin & Carter, 1970.

Diagnosis. – Pattern H or H' rhabdosome with glyptograptid to orthograptid thecae throughout, with no thickening of the genicula; rhabdosome widens gradually from the proximal end (Melchin *et al.* 2011).

***Korenograptus laciniosus* (Churkin & Carter, 1970)**
Figure 6D

*1970 *Glyptograptus laciniosus* Churkin & Carter; pp. 26–27, text-fig. 11D; pl. 2, figs 17, 18.
v. 2005 *Normalograptus laciniosus* Churkin & Carter. – Chen *et al.*, pp. 259–260, pl. 1, figs 3, 5, 6; text-fig. 8K [see for synonymy list].
? 2005 *Normalograptus laciniosus* Churkin & Carter. – Chen *et al.*, pp. 259–260, text-figs 7E, 8A, P, V, X, Z.
2006 *Normalograptus laciniosus* Churkin & Carter. – Chen *et al.*, text-fig. 9-31, 32.
2007 *Normalograptus laciniosus* Churkin & Carter. – Chen *et al.*, text-fig. 3Z; text-fig. 4M.
2011 *Korenograptus laciniosus* (Churkin & Carter). – Melchin *et al.*, p. 301.

Material. – Twenty-five specimens: six from the Dawangou section, the others from the Dawangou East section.

Description. – Rhabdosome up to 15.4 mm long, widening from 0.8–0.9 mm at the first thecal pair to the maximum width of 1.2–1.5 mm distally. 2TRD is 1.3–1.7 mm at th2^1, 1.4–1.6 mm distally. Thecae are glyptograptid with flowing genicula. The apertures are horizontal. Th1^1 turns upward slightly below the sicular aperture with an upward-growing portion 0.8–0.9 mm long. Th1^2 crosses the sicula diagonally, leaving the dorsal side of the sicula exposed for *ca* 0.4–0.55 mm. The median septum is full, originating at least at the second thecal pair.

Figure 3. A, D – *Avitograptus* sp. aff. *A. avitus* (Davies, 1929); A – XKDE2-0.3-19; D – KD-HB-48-07. • B, G – *Hirsutograptus jideliensis* (Koren' & Mikhaylova *in* Koren' *et al.*, 1980); B – XKT1-75-3; G – XKT1-57-1. • I, K – *Korenograptus* aff. *K. magnus* (Churkin & Carter, 1970); I – XAS50-20; K – XAS50-56. • E, F, J, L, M, O, R, T – *Metabolograptus parvulus* (H. Lapworth, 1900); E – XKT1-42-1; F – XKT1-28-1; J – DMK2-1.1-2; L – KD-hb-48-10; M – XKDE 2-66; O – XKT1-37; R – XKT1-41-1; T, XKT1-33-1a); C, H, N, P, Q, U, V – *Persculptograptus* sp.; C – XKT1-7-4; H – XAS50-14; N – XKT1-76-1; Q – XAS50-44d; U – XAS50-31; V – XAS50-17; P – XKT1-68. • S – *Normalograptus angustus* (Perner, 1895); XKT1-60. All scale bars represent 1 mm. A, C, D, E, F, H, J, M, N, P–V, magnification × 10; B, G, L, O, magnification × 8; I, K, magnification × 6.


A
B
C
D
E
F
G
H
I
J
K
L
M
N
O
P
Q
R
S
T
U
V

Discussion. – The present specimens resemble the type material in size and show the characteristic thecal shape. The specimens described herein differ from those reported from the Yangtze region by Chen *et al*. (2005) in having a narrower rhabdosome width and a slightly tapering proximal end.

Stratigraphical range. – In Alaska, this species occurs from the *Pk. acuminatus* to the *C. gregarius* biozones (Churkin & Carter 1970); it has been recorded from the upper *D. mirus* Biozone to *Ak. ascensus* biozones in the Yangtze region in China (Chen *et al*. 2005).

***Korenograptus* aff. *K. magnus* (Churkin & Carter, 1970)**
Figure 3I, K

aff.*1970 *Glyptograptus tamariscus magnus* Churkin & Carter; pp. 26–27, text-fig. 11D; pl. 2, figs 17, 18.
non 1984 *Glyptograptus tamariscus magnus* Churkin & Carter. – Lin & Chen, p. 211, pl. 1, fig. 7; pl. 2, figs 1–7.
1990 *Glyptograptus rigidus* Fang *et al*., pp. 60–61, pl. 9, figs 9, 12.

Material. – Three specimens from the Sishichang section.

Description. – Rhabdosome up to 20 mm long, widening from 0.60–0.80 mm at the first thecal pair to a maximum width of 1.6–1.8 mm distally. The 2TRD is 1.6–1.7 mm at $th2^1$, 1.7–1.9 mm distally. Thecae vary throughout the rhabdosome: the sigmoidal curvature is strong proximally but decreases distally, with rounded, flowing genicula. The excavations become longer and more open while the genicular wall becomes relatively short in length distally. The apertures are horizontal. $Th1^1$ turns upward slightly below the sicular aperture with an upward-grown portion 0.9–0.95 mm long. The sicula is exposed for *ca* 0.35–0.45 mm below $th1^2$. The virgella is stout and reaches a length of 3.8 mm. There is a full median septum, originating at least at the second thecal pair.

Discussion. – These specimens have long and smoothly tapering rhabdosomes that resemble the type material in overall shape. $Th1^1$ turns upward slightly below the sicular aperture in the present specimens, recalling the transmitted infrared microscopy image of *K. magnus* provided by Melchin *et al*. (2011, fig. 5I), which showed a downward-grown $th1^1$ terminating in two foramina. However, our material differs from the types in having a tapering, less elongate proximal end and a lesser rhabdosome width. The Tarim specimens differ from those from Cape Manning, Nunavut, Canada illustrated by Melchin *et al*. (2011) in having a sharper geniculum on the proximal thecae and shorter supragenicular walls. Another species, *Korenograptus*? *praecursor* (Koren' & Rickards 2004), only questionably assigned to *Korenograptus* by Melchin *et al*. (2011), has relatively sharp genicula and slight genicular thickenings. The Tarim specimens differ from that species in having a greater maximum width.

Stratigraphical range. – In Alaska, *K. magnus* occurs in the *Co. cyphus* Biozone (Churkin & Carter 1970). *G. rigidus* has been reported from the *Cy. vesiculosus* to *Co. cyphus* biozones of Jiangxi Province, south China by Fang *et al*. (1990).

***Korenograptus jerini* (Koren' & Melchin, 2000)**
Figures 4K, T, W, Y, 7K

*2000 "*Glyptograptus*" *jerini* Koren' & Melchin, p. 1107, text-figs 9.7, 9.8, 9.20, 11.4–11.6.
2007 *Normalograptus jerini* (Koren' & Melchin). – Chen *et al*., pp. 80, 81, text-fig. 3S, text-fig. 4H.

Material. – Twenty-nine specimens: three from the Sishichang section, 15 from the Tierekeawati section, and 11 from the Dawangou East section.

Description. – Rhabdosome up to 12.82 mm long. It widens from 0.7–0.85 mm at the first thecal pair to a maximum width of 1.0–1.25 mm distally. The 2TRD is 1.3–1.4 mm at $th2^1$, 1.5–1.7 mm distally. Thecae are biform: climacograptid thecae with distinct genicula are present proximally, becoming glyptograptid thecae with flowing genicula distally. The apertures are horizontal. Sicula is 1.5–1.75 mm long. $Th1^1$ first grows downward and then turns upward 0.1–0.15 mm below the sicular aperture, with an upward-growing portion 0.85–0.90 mm long. $Th1^2$ crosses the sicula diagonally, leaving the dorsal side of

Figure 4. B, C, D, F, O – *Normalograptus ajjeri* (Legrand, 1977); B – XKDE2-62; C – XKT1-23-1; D – XKT1-17; F – XKT1-33-2a; O – XKT1-14-2). • A, E, G, H, J, L, M, R, X – *Normalograptus mirnyensis* (Obut & Sobolevskaya *in* Obut *et al*., 1967); A – XAS50-57; E – XKT1-51-1; G – XKT1-1; H – XKT1-13-2; J – XKT1-19-3; L – XKT1-10-2; M – XKT 1-49a; R – XKT1-9; X – DKM2-0.5-36. • I – *Normalograptus angustus* (Perner, 1895); XKT1-58. • K, T, W, Y – *Korenograptus jerini* (Koren' & Melchin, 2000); K – XKT1-7-1; T – XKDE2-2a-1; W – XKT1-66-2; Y – XKT1-7-3. • N, P, Q, S, U, V – *Metabolograptus wangjiawanensis* (Mu & Lin, 1984); N – XAS50-35; P – XAS50-22; Q – XKDE2-28a-1; S – XAS50-46a-2; U – XAS50-1b; V – XAS50-27c. All scale bars represent 1 mm. A, B, D, E, G, H, I, J, M, O, Q, R, magnification × 10; C, F, K, L, N, P, T–Y, magnification × 8; S, magnification × 6.

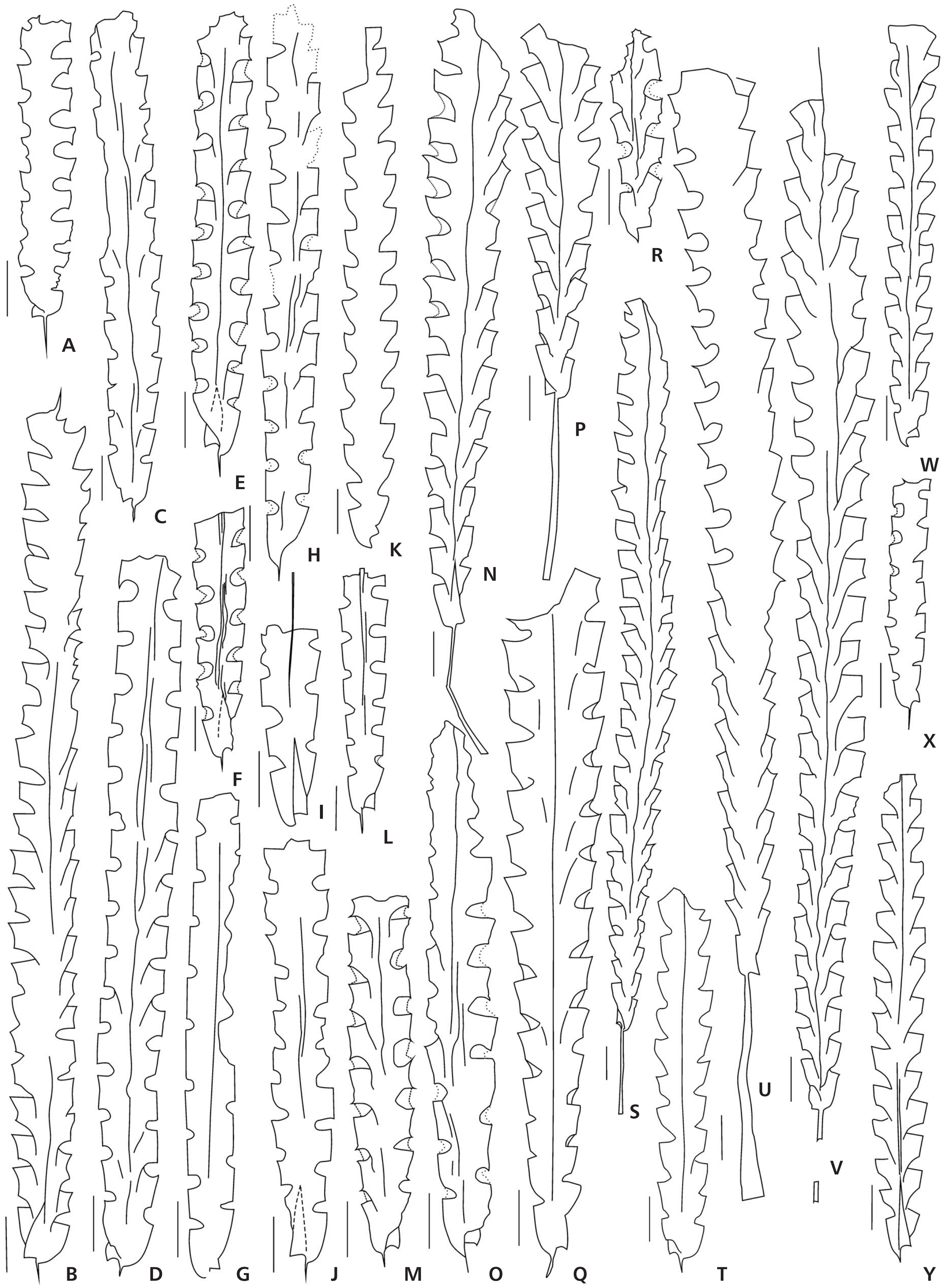
A
B
C
D
E
F
G
H
I
J
K
L
M
N
O
P
Q
R
S
T
U
V
W
X
Y

Table 2. Morphometric details of *Metabolograptus parvulus* from the Tarim Region and comparative regions. *DVW: dorso-ventral width.

Species	Locality	Reference	DVWth1	Distal DVW/mm	2TRD th1/mm	2TRD th5/mm	Distal 2TRD/2TRD th10
N. parvulus	Type locality: Rhayader district, Wales, UK	Lapworth (1900)	0.8–0.9	1.1–1.5	1.4	1.5–1.7	1.5–1.8
N. parvulus	Anticosti, Canada	Melchin (2008)	0.9	1.5	1.3	1.6	1.7
N. parvulus	Jordan	Loydell (2007)	0.7–1.0	1.25–1.7	1.15–1.65	1.25–1.8	1.45–1.7
M. parvulus	Tarim, China	This paper	0.7–0.9	1.0–1.4	1.3–1.5	1.3–1.4	1.4–1.7
N. aff. *N. parvulus*	Wales, UK	Blackett *et al.* (2008)	0.6–1.0	0.9–1.2	1.5–2.2	1.7–2.4	1.9
N. cf. *parvulus*	Wales, UK	Blackett *et al.* (2008)	0.7–1.0	0.9–1.8	1.1–1.6	1.4–1.8	1.5–1.9
N. parvulus	Yangtze Region, South China	Chen *et al.* (2005)	0.95–1.15	1.4–1.7	1.35–1.7		1.6–1.9
N. parvulus	Illinois and Iowa, USA	Loydell *et al.* (2002)	0.8–0.95	1.25–1.75	1.15–1.6	1.4–1.55	1.5–1.75

the sicula exposed for *ca* 0.3–0.4 mm. The median septum can be observed to originate at the third thecal pair.

Discussion. – The present specimens show typical glyptograptid thecae distally combined with normalograptid Pattern H early astogeny. *Korenograptus jerini* shows great similarity to *N. elegantulus* (Mu & Ni, 1983), which also possesses biform thecae, but differs from the latter in having a narrower rhabdosome and more densely spaced thecae. When compared with the type material from the Urubulak Formation of Uzbekistan, the median septum appears to originate closer to the proximal end in the present specimens.

Stratigraphical range. – *Korenograptus jerini* is recorded from the *A. cuneatus* and *H. sinitzini* subzones (*Ak. ascensus–Pk. acuminatus* Biozone) in the Kurama Range, Eastern Uzbekistan (Koren' & Melchin 2000) and the *Ak. ascensus* Biozone of northwestern Zhejiang, China (Chen *et al.* 2007).

Genus *Metabolograptus* Obut & Sennikov, 1985, emend. Melchin *et al.*, 2011

Type species. – *Diplograptus modestus sibericus* Obut, 1955.

Diagnosis. – The partial clade that includes Pattern H species with sharp to bluntly rounded genicula, a gently sinuous median septum proximally, sinuous interthecal septa, subapertural walls parallel to moderately inclined (Melchin *et al.* 2011).

Discussion. – *Metabolograptus* was erected by Obut & Sennikov (1985) with *Metabolograptus sibericus* as the type species. This genus contains Hirnantian–early Silurian graptolite species with biform thecae. The thecae undergo a transition from climacograptid type proximally to glyptograptid type distally. The assignment of *M. extraordinarius*, *M. parvulus*, and *M. ojsuensis* to *Metabolograptus* is becoming widely accepted (*e.g.*, Štorch & Schönlaub 2012, Cooper *et al.* 2014, Maletz 2014, Kraft *et al.* 2015).

Metabolograptus parvulus (Lapworth, 1900)

Figures 3E, F, J, L, M, O, R, T, 7J, 8B, E, F

* 1900 *Climacograptus parvulus* H. Lapworth, p. 132, fig. 20a–c.
p. ?1986 *Glyptograptus persculptus* group; Berry, p. 140, fig. 5h–i? [non fig. 5g, j].
1991 *Glyptograptus* cf. *G. persculptus* (Williams). – Melchin *et al.*, p. 1856.
.2006 *Normalograptus parvulus* (H. Lapworth). – Chen *et al.*, p. 190, text-figs 9, 11.
2007 *Normalograptus parvulus* (H. Lapworth). – Loydell, pl. 2, figs 5, 9; text-figs 18I, J, L, M, O [see for synonymy list].
.2008 *Normalograptus parvulus* (H. Lapworth). – Melchin, pp. 157, 158, 159, 160, text-figs 4A, B.
? 2008 *Normalograptus* cf. *N. parvulus* (H. Lapworth). – Melchin, p. 157, text-fig. 2B.
.2008 *Normalograptus parvulus* (H. Lapworth). – Blackett *et al.*, p. 89, text-fig. 5Q.
aff. 2008 *Normalograptus*? aff. *parvulus* (H. Lapworth). – Blackett *et al.*, p. 89, text-figs 5F–M.
cf. 2008 *Normalograptus*? cf. *parvulus* (H. Lapworth). – Blackett *et al.*, p. 89, text-fig. 5N.
2011 *Metabolograptus parvulus* (H. Lapworth). – Melchin *et al.*, p. 296.

Material and stratigraphical range. – Eighteen specimens: 12 from the Tierekeawati section, four from the Dawangou section and two from the Dawangou East section.

Description. – The rhabdosome widens from 0.7–0.9 mm at the first thecal pair to the maximum width of 1.0–1.4 mm distally. The thecae have sharp, non-hooded genicula. The supragenicular walls are straight and with a slight inclination. The 2TRD is 1.3–1.5 mm at the proximal end, 1.4–1.7 mm distally. $Th1^1$ first grows downward and then turns upward just below the sicular aperture. The upward-growing portion of theca 1^1 is 0.8–1.0 mm long. $Th1^2$ crosses the sicula almost immediately above the sicular aperture, leaving little exposure of the sicular wall below $th1^2$. Some specimens show an undulose median septum that originates as early as the first thecal pair. Relatively long, undulose interthecal septa can be observed clearly near the proximal end.

Discussion. – *Metabolograptus parvulus* is characterized by its close thecal spacing, undulose median septum, sinuous interthecal septa, and relatively short thecal supragenicular walls. It is frequently associated with *Persculptograptus persculptus*, and differs from the latter in having more densely spaced thecae and a lesser maximum rhabdosome width. *M. parvulus* can be distinguished from *Avitograptus* sp. aff. *A. avitus* from Tarim by the significantly elongated proximal thecae of the latter.

The present specimens of *M. parvulus* match well those reported from central Wales by Zalasiewicz & Tunnicliff (1994) and Blackett *et al*. (2008), and from Anticosti Island (first by Riva (1988) as *N. angustus*; later, Zalaziewicz & Tunnicliff (1994), Chen *et al*. (2005), Loydell (2007), and Melchin (2008) considered some of the Anticosti specimens to be *M. parvulus*). Flattened specimens of *M. parvulus* from the Yangtze Region, China (Chen *et al.* 2005) show little exposure of the sicular wall below $th1^2$ and a greater rhabdosome width than the present specimens. Isolated specimens from Iowa, USA, illustrated by Loydell *et al*. (2002) show an inclined supergenicular wall and introverted apertural margins, which were also observed in this study. Melchin (2008) distinguished two species, *Metabolograptus parvulus* and *Normalograptus* cf. *N. parvulus*, when he re-examined the collections of Riva (1988) together with new specimens. The latter material was left in open nomenclature because of the sub-parallel-sided nature of the rhabdosome. Blackett *et al*. (2008) illustrated graptolites from two sites in central Wales. They distinguished two morphological types: *N.*? aff. *parvulus* with noticably greater 2TRD and *N.*? cf. *parvulus* with sub-parallel-sided rhabdosomes and a slightly larger size.

Stratigraphical range. – *M. parvulus* is restricted to the *P. persculptus* to lower *Pk. acuminatus* biozones in central Wales and southern Scotland (Williams 1983, Zalasiewicz & Tunnicliff 1994, Blackett *et al*. 2008). It is known from the *P. persculptus* Biozone in Arctic Canada, Anticosti Island, and the Yangtze region of China (Melchin *et al*. 1991, Chen *et al*. 2005, Melchin 2008). It has been recorded throughout the *Ak. ascensus–Pk. acuminatus* Biozone and possibly higher in Jordan (Loydell 2007).

Metabolograptus wangjiawanensis **(Mu & Lin, 1984)**
Figures 4N, P, Q, S, U, V, 6B, G, H, 7B

*1984 *Climacograptus wangjiawanensis* Mu & Lin, p. 59, pl. 4, figs 10, 11.
1985 *Normalograptus wangjiawanensis* (Mu & Lin, 1984). – Chen *et al.*, p. 269, pl. 2, fig. 6, text-figs 10C, K, P, T, U [see for synonymy list].
2007 *Normalograptus wangjiawanensis* (Mu & Lin). – Chen *et al*., p. 80, text-fig. 3AA.

Material and stratigraphical range. – Ten well-preserved specimens: five from the Sishichang section and five from the Dawangou East section.

Description. – The rhabdosome is up to 26 mm long, widening from 0.65–0.90 mm at the first thecal pair to a maximum width of 1.7–2.0 mm distally. Thecae have sharp, thickened genicula. The supragenicular walls are slightly inclined and apertures are horizontal. The infragenicular wall is strongly sigmoidally curved. 2TRD is 1.5–1.95 mm at $th2^1$, 1.75–2.25 mm distally. $Th1^1$ first grows downward and then turns upward just below the sicular aperture. The upward-growing portion of $th1^1$ is 0.75–0.9 mm long. $Th1^2$ crosses the sicula diagonally, leaving the dorsal side of the sicula exposed for 0.3–0.55 mm. The virgella is long and robust, 2.6–5.5 mm long, sometimes widening to form a vane shape or a spatulate structure. The median septum is undulose proximally and gradually straightens distally. Its origination position varies from the first thecal pair to the third or fifth thecal pair.

Discussion. – Many Upper Ordovician and lower Silurian graptolite species bear long and robust virgellae. *Metabolograptus wangjiawanensis* and *Climacograptus caudatus* Lapworth, 1876 differ in the shape of the virgella distally: that of the former widens to a spatulate structure, whereas that of the latter widens to a fan shape. *Climacograptus antiquus bursifer* Elles & Wood has a robust virgella as well as a pair of thecal spines from the first theca. *Climacograptus antiquus bursifer* and *Climacograptus wilsoni* Lapworth, 1876 have a membrane surrounding the virgella. *Normalograptus rhizinus* (Li & Yang *in* Nanjing Institute of Geology and Mineral Resources, 1983) also possesses a widened virgella distally. The material described herein differs from *Normalograptus rhizinus* in the smaller length of supragenicular wall, larger rhabdosome width, and closer thecal spacing. The material differs from another Chinese species, *Climacograptus bidongensis* Fu, 1982, in having a narrower rhabdosome and longer exposure of the antivirgellar side under $th1^2$. The present species also resembles *Korenograptus jerini* from the Urubulak Formation (*A. cuneatus* and *H. sinitzini* subzones) of Uzbekistan, reported by Koren' & Melchin (2000), in which the median

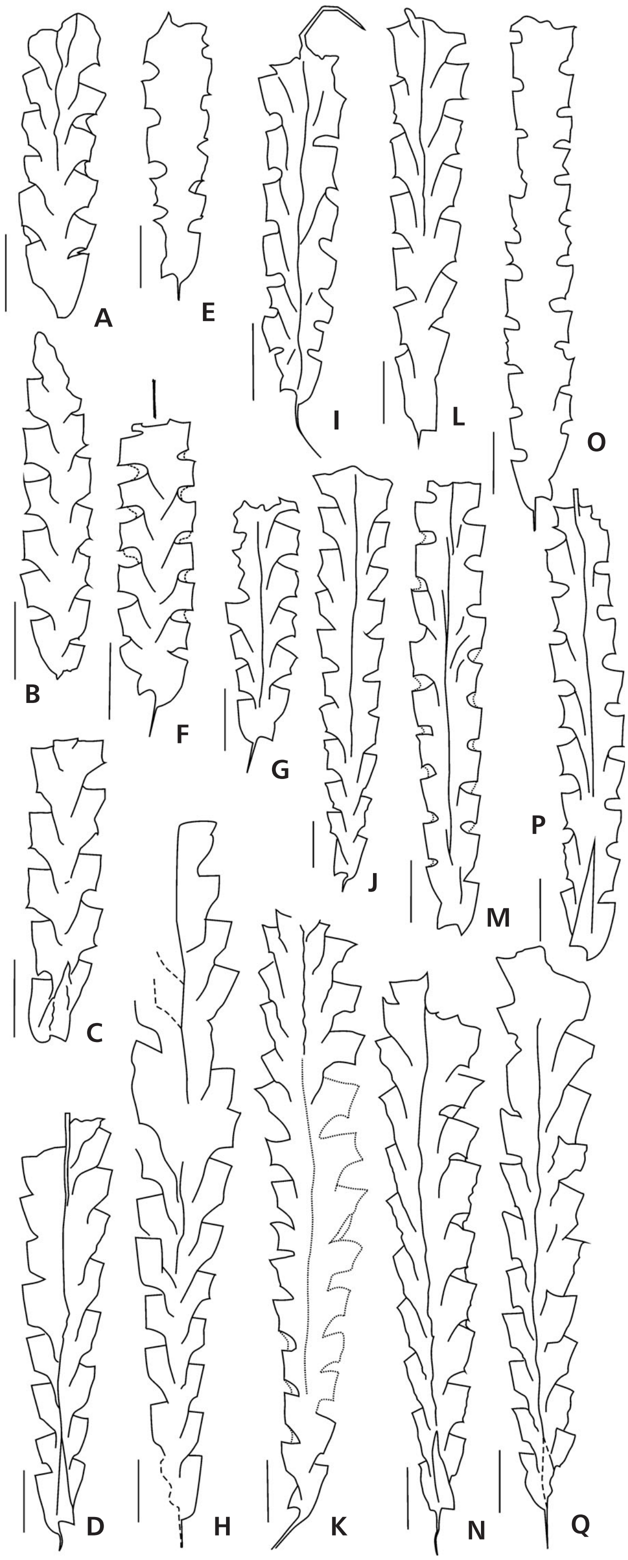

Figure 5. A, E, F, G, M, O, P – *Hirsutograptus jideliensis* (Koren' & Mikhaylova *in* Koren' *et al*., 1980); A – XKT1-13-2; E – XKT1-70-5; F – DKM2-0.4-8; G – XKT1-66-4; M – KD-HB-48-03; O – XKT1-16-2; P – XKT1-42-1. • B, C, I – *Paramplexograptus madernii* (Koren' & Mikhaylova *in* Koren' *et al*., 1980); B – HD-HB-48-21; C – DKM2-1.6-30; I – KD-HB-48-03. • D, H, J, K, L, N, Q – *Paramplexograptus*? sp.; D – XAS50-13; H – XKDE1-1; J – XAS50-28A-2; K – XAS50-37; L – XKDE2-64-1; N – XAS50-46; Q – XKT1-75-3. All scale bars represent 1 mm. A, B, C, F, I, magnification × 10; D, E, G, H, K–P, magnification × 8; J, magnification × 6.

septum also originates from the fourth or fifth thecal pair but differs in having a greater maximum width and sharply geniculate thecae throughout the rhabdosome. *Metabolograptus wangjiawanensis* is reported to have a wide range of variation in maximum width. The maximum width of the holotype is 2.4–2.5 mm. A later report by Chen *et al*. (2005) stated that this species has a width range of 1.9–2.2 mm. Due to the preservation of the type collection, the origination of the median septum of *M. wangjiawanensis* is hard to discern. However, the median septum may begin around the third thecal pair (Dr M. Melchin, pers. comm.). Combined with the data from the present study, *M. wangjiawanensis* may have a delayed median septum that originates around the 3rd to 5th thecal pair.

Stratigraphical range. – In the Yangtze region of South China, *M. wangjiawanensis* is reported from the *P. persculptus* Biozone to the *Ak. ascensus* Biozone (Chen *et al*. 2005). In Arctic Canada, it has been recorded from the *P. persculptus* Biozone (Melchin *et al*. 1991).

Genus *Persculptograptus* Koren' & Rickards, 1996

Type species. – *Glyptograptus persculptus* Elles & Wood, 1907.

Diagnosis. – Robust biserial graptoloids, septate to aseptate, up to 40 mm long and with a distal dorso-ventral width sometimes in excess of 2.5 mm (in specimens preserved in relief); proximal development normal Pattern (H); thecae doubly sigmoidal with slight geniculum in the proximal thecae of some species; thecal overlap considerable; median septum commonly undulating in the proximal region, less so distally; sicula of moderate length, often well exposed in reverse view; virgellate, virgella usually short, spike-like nema expanded slightly distally (Koren' & Rickards 1996).

Discussion. – Koren' & Rickards (1996) erected the genus *Persculptograptus* and assigned *Persculptograptus persculptus*, which has characteristic doubly sigmoidal thecae, as the type species. *Persculptograptus* was treated as a junior synonym of *Metabolograptus* in the phylogenetic study of Melchin *et al*. (2011). They suggested that *P. persculptus* together with *M. sibericus*, *N. ojsuensis*, *N. extraordinarius* and *N. parvulus* be included in *Metabolograptus*. However, Obut & Sennikov (1985) had realized that

P. persculptus has different features (doubly sigmoidal thecae, considerable thecal overlap and a proximally undulating median septum), and thus did not transfer it to *Metabolograptus*. In this study, we prefer to retain *Persculptograptus* as a separate genus.

***Persculptograptus* sp.**
Figures 3C, H, N, P, Q, U, V, 6A, C, E, F, 7C

Material. – Fifteen specimens: seven from the Sishichang section, five from the Tierekeawati section, and three from the Dawangou East section.

Description. – The rhabdosome widens from 0.9 mm at the first thecal pair to a maximum width of 1.8–2.3 mm distally. The proximal thecae are climacograptid with sharp, non-hooded genicula. Distal thecae are moderately to gently sigmoidal. The supragenicular walls are straight and inclined slightly. The specimens have relatively short supragenicular walls (measuring 0.6 mm at $th4^1$ and 0.55 mm at $th8^1$) and large apertural excavations (around 0.5 mm at $th4^1$ and $th8^1$). 2TRD is 1.6–1.7 mm at $th2^1$, 1.9 mm distally. The sicula is 1.3 mm long and bears a short, robust virgella. $Th1^1$ first grows downward and then turns upward just below the sicular aperture. The upward-growing portion of $th1^1$ is 0.9–1.0 mm long. Some specimens show an undulose median septum proximally, which gradually becomes straight distally. The median septum is nearly complete, and originates as early as the first thecal pair.

Discussion. – The present material resembles the type specimens of *P. persculptus* in having sharp-flowing genicula, an undulose median septum, and sinuous interthecal septa. The present specimens differ from *M. parvulus* in having greater rhabdosome width and 2TRD value both proximally and distally. The material described herein can be distinguished from *M. ojsuensis* in having a narrower proximal end, a smaller distal 2TRD value, shorter infragenicular walls, and taller apertural excavations. The present specimens, which are preserved in partial relief, have a relatively smaller rhabdosome width (maximum width 1.8 mm in partial relief), thus resembling *P. persculptus* from Bornholm, Denmark (maximum width 1.6 mm in full relief, 2.0 mm in flattened specimens; Bjerreskov 1975). *Persculptograptus* sp. can be distinguished from *P. persculptus* by the fact that the latter has much smaller apertural excavations and relatively much longer supragenicular walls. Blackett *et al.* (2008) performed a morphometric analysis on graptolites from several localities in Wales; their detailed biostratigraphical subdivision of the *P. persculptus* to *Pk. acuminatus* biozones was principally based on the delay in the insertion point of the median septum. The youngest interval in the mid-*acuminatus* Biozone contains *Persculptograptus* cf. *persculptus*, which does not display a median septum on its reverse side. The specimens of *Persculptograptus* cf. *persculptus* from Wales described by Blackett *et al.* (2008) have similar DVW and 2TRD values to *P.* sp. and relatively short and slightly inclined supragenicular walls. Davies (1929) originally suggested that stratigraphically later forms of *Persculptograptus* show late insertion of the median septum.

Family Retiolitidae Lapworth, 1873, emend.
Melchin *et al.*, 2011
Paraphyletic subfamily Petalolithinae Bulman, 1955, emend. Melchin *et al.*, 2011

Genus *Paramplexograptus* Melchin *et al.*, 2011

Type species. – *Paraorthograptus paucispinus* Li, *in* Anhui Geological Survey Team (1982).

Diagnosis. – Species that form an aseptate rhabdosome with Pattern H’ or Pattern I proximal structure and the nema attached to the base of the interthecal septa. Thecae have sharp genicula with thickenings or ventral flanges, and slightly to moderately inclined, usually concave subapertural walls. The sicular aperture shows a slight dorsal flare (Melchin *et al.* 2011).

***Paramplexograptus madernii* (Koren’ & Mikhaylova *in* Koren’ *et al.*, 1980)**
Figures 5B, C, I, 8I

*1980 *Glyptograptus madernii* Koren’ & Mikhaylova *in* Koren’ *et al.*, pp. 141–143, pl. XL, figs 3–9; text-fig. 42α–ε.

v. 2005 *Normalograptus* sp. aff. *N. indivisus* (Davies). – Chen *et al.*, pp. 270, 271; pl. 2, fig. 10; text-figs 10A, E–F, M.

2007 *Normalograptus madernii* (Koren’ & Mikhaylova). – Chen *et al.*, pp. 80, 81, text-fig. 3V.

.2011 *Paramplexograptus madernii* (Koren’ & Mikhaylova). – Melchin *et al.*, pp. 299, 301, text-fig. 5B.

Material. – Eight specimens: six from the Dawangou East section and two from the Dawangou section.

Description. – The rhabdosome is up to 5.9 mm long. It widens from 0.75–0.8 mm at the first thecal pair to 0.9–1.15 mm at the sixth, and retains this width to the distal end of the rhabdosome. The 2TRD is 1.15–1.45 mm at $th2^1$ and 1.3–1.5 at $th6^1$. The descending portion of the first theca is 0.5 mm long. Theca 1^1 turns upward just below the base of the sicula and $th1^2$ crosses the sicula diagonally, leaving the dorsal side of the sicula exposed for *ca* 0.35–0.45 mm. The rhabdosome is aseptate. Thecae are of climacograptid type with parallel-sided to slightly concave supragenicular walls and straight but oblique apertural margins. The genicula are sharp and show thickened rims around the genicula, sometimes forming small genicular flanges. The apertural excavations are large, and the ratio between the supragenicular wall and the excavation at th5^1 is around 2:1.

Discussion. – The present specimens are aseptate. The Chinese specimens that were identified as *N.* sp. aff. *N. indivisus* (Waern, 1948) from the Yangtze Region by Chen *et al.* (2005) are clearly aseptate with alternate thecae throughout. Moreover, one of those specimens (Chen *et al.* 2005, text-fig. 10A) shows that the bases of the interthecal septa are attached to the nema. These specimens differ from *N. indivisus*, which also has a dicalycal theca and two separate stipes distally, and are regarded as *Paramplexograptus madernii* herein.

The present specimens fit well with the definition of *Paramplexograptus* Melchin *et al.* (2011). *Paramplexograptus* contains species that are aseptate, with a Pattern H' or Pattern I proximal structure and with the bases of the interthecal septa attached to the nema. These characters help to separate *Paramplexograptus madernii* from the hooded form of *Hirsutograptus jideliensis* (Koren' & Mikhaylova *in* Koren' *et al.*, 1980).

Stratigraphical range. – *Paramplexograptus madernii* was first reported from the *Pk. acuminatus* Biozone in Kazakhstan (Koren' & Mikhaylova *in* Koren' *et al.* 1980).

Subsequently it was recorded in the *P. persculptus* Biozone of the Yangtze Region of South China (as *Normalograptus* sp. aff. *N. indivisus* by Chen *et al.* 2005); recently, it has been reported throughout the *M. extraordinarius*, *P. persculptus*, and *Ak. ascensus* biozones of Northwestern Zhejiang, China (Chen *et al.* 2007).

Paramplexograptus? sp.

Figures 5D, H, J, K, L, N, Q, 7 D, F, H, I

v ? 2005 *Normalograptus avitus* (Davies, 1929). – Chen *et al.*, pl. 1, fig. 11, pl. 2, fig. 9, text-figs 7D, G, J–L.

Material. – Eleven specimens: five from the Dawangou East section, five from the Sishichang section, and one from the Tierekeawati section.

Description. – The rhabdosome widens from 0.7–0.8 mm at the first thecal pair to a maximum width of 1.65 mm at the sixth/seventh thecal pair, and retains this width to the distal end of rhabdosome. The 2TRD is 1.5–1.9 mm at th2^1 and 1.4–1.8 at th10^1. The virgella is short, around 0.3–1 mm long. Th1^1 turns upward just below the base of the sicula and th1^2 crosses the sicula diagonally, leaving the antivirgellar side of the sicula exposed for *ca* 0.15–0.45 mm; the ascending length of th1^1 is 0.8–1.1 mm. The rhabdosome is aseptate proximally and with alternate thecae in the first three to four thecal pairs. The genicula are sharp and show thickened rims around the genicula. The bases of the interthecal septa are attached to the nema.

Discussion. – The species has a cuneiform shape at the proximal end, and the first several thecae grow alternately. Whether this species has a median septum is uncertain. Some of the specimens (*e.g.*, Fig. 5D) show that the bases of the interthecal septa are attached to the nema. The present material shows a tendency for elongation in the first thecal pair and long exposure of the sicula below th1^2: this recalls *Avitograptus avitus*. However, the present material differs from *A. avitus* in having a larger proximal width and a less elongate first thecal pair. The great similarity between the specimens tentatively suggests an assignment to *Paramplexograptus*.

Paraphyletic family Normalograptidae Štorch & Serpagli, 1993, emend. Melchin *et al.*, 2011

Genus *Normalograptus* Legrand, 1987, emend. Melchin *et al.*, 2011

Type species. – *Normalograptus scalaris* var. *normalis* Lapworth, 1877; by original designation.

Diagnosis. – Species with Pattern H rhabdosomes that possess unornamented climacograptid thecae with straight or concave interthecal septa throughout the rhabdosome and a full median septum, which may be delayed (Melchin *et al.* 2011).

Normalograptus ajjeri (Legrand, 1977)

Figures 4B, C, D, F, O, 8H

*1977 *Climacograptus (Climacograptus) normalis ajjeri* Legrand, p. 171, text-figs 9A–D, 10A, B.

Figure 6. A, C, E, F – *Persculptograptus* sp.; A, C – XAS50-17; E – XAS50-39; F – XKT1-76-1. • D – *Korenograptus laciniosus* (Churkin & Carter, 1970); DKM2-1.1-24. • B, G, H – *Metabolograptus wangjiawanensis* (Mu & Lin, 1984); B – XAS50-22; G – XAS50-1; H – XAS50-46a. All scale bars represent 1 mm.


A
B
C
D
E
F
G
H

.1984 *Climacograptus normalis* Lapworth. – Chen, p. 40; pl. 2, figs 15, 16; pl. 3, fig. 1; text-fig. 3i.
1984 *Climacograptus pseudonormalis* Li, p. 346, pl. 14, figs 10, 13–17.
1995 *Climacograptus pseudonormalis* Li, p. 241, pl. 3, fig. 20; pl. 8, figs 1–6, 8; pl. 26, fig. 11.
1999 *Normalograptus normalis* (Lapworth). – Li, p. 95, pl. 1, fig. 18.
2000 *Normalograptus normalis* (Lapworth). – Koren' & Melchin, p. 1101, fig. 7.14.
v? 2005 *Normalograptus normalis* (Lapworth). – Chen *et al.*, p. 264, text-fig. 9J.
.2007 *Normalograptus ajjeri* (Legrand). – Loydell, pp. 29, 30, text-figs 12G, 15A–F, H–I, O [see for synonymy list].
.2008 *Normalograptus ajjeri* (Legrand). – Štorch & Feist, p. 943, text-figs 6.14, 7.22.
.2011 *Normalograptus ajjeri* (Legrand). – Štorch *et al.*, pp. 368, 369, figs 25B–D, P, V, W, 26L, M.
.2012 *Normalograptus ajjeri* (Legrand). – Štorch & Schönlaub, p. 759, figs 3A, B, ?D, ?O, 4E, F.

Material. – Twenty specimens: nineteen from the Tierekeawati section and one from the Dawangou East section.

Description. – The rhabdosome is more than 14.0 mm long. It measures about 0.8–0.9 mm in dorso-ventral width at the first thecal pair, and widens gradually to its maximum width of 1.4–1.6 mm. The rhabdosome is parallel-sided for most of its length. 2TRD is 1.4–1.8 mm at $th2^1$ and 1.6–1.9 mm distally. The thecae are climacograptid in form and sub-alternating. The supragenicular walls are straight, with sharp and obvious genicula. The apertures are horizontal and open into semicircular excavations. The proximal end is asymmetrical; the virgella is short and sometimes more than 0.5 mm long. $Th1^1$ first descends and then turns upward just below the sicular aperture. The upward-grown portion of $th1^1$ is 0.8–1.0 mm long. $Th1^2$ crosses the sicula high above the sicular aperture and leaves the sicular wall below $th1^2$ free for 0.2–0.4 mm. A full median septum is developed.

Discussion. – The thecal form is the typical box-like "*scalaris*" form. The dimensions of the material match well those of the Jordanian material described by Loydell (2007), except that the maximum rhabdosome width of the Jordanian material is very slightly smaller. Loydell (2007) re-examined the type material of *N. normalis* and found it to be significantly broader (1.85–2.05 mm in maximum width without significant preservational effects) than the specimens generally assigned to this species previously. He suggested that many narrower forms should be reassigned to *N. ajjeri*, a similar species with narrower width. This idea obtained some support from Štorch & Schönlaub (2012). One of the Chinese *N. normalis* specimens from the Yangtze region has a relatively wide and blunt proximal end and a small rhabdosome width, which may suggest a close relationship to *N. ajjeri* (Chen *et al.* 2005, text-fig. 9J). However, $th1^2$ of the Yangtze region specimen crosses the sicula just above the sicular aperture. These features separate this specimen from typical *N. ajjeri*, which has a larger amount of the sicular wall exposed below $th1^2$.

Melchin *et al.* (2011) restricted *Normalograptus* to include only species with parallel, unornamented thecae (*e.g.*, *N. normalis*, *N. ajjeri*, *N. angustus*), because their phylogenetic analysis found that that all of the species previously included in this genus that possessed either inclined thecae (*M. parvulus*, *K. laciniosus*) or genicular hoods (*H. jideliensis*) were more closely related to the type species of other genera (*e.g.*, *Metabolograptus*, *Hirsutograptus*, *Korenograptus* or *Neodiplograptus*) than they were to *Normalograptus normalis*.

Stratigraphical range. – *N. ajjeri* has a long stratigraphical range; it has been recorded from the Hirnantian through to the lower Aeronian (Loydell 2007). In the Yangtze region, the species has been reported from the upper *P. pacificus* Biozone to the *M. extraordinarius* Biozone (in part as *N. normalis* by Chen *et al.* 2005).

***Normalograptus angustus* (Perner, 1895)**
Figures 3S, 4I, 8G, J

*1895 *Diplograptus (Glyptograptus) euglyphus angustus* Perner, p. 27, pl. 8, fig. 14a, b.
1975 *Climacograptus angustus* (Perner). – Bjerreskov, p. 23, fig. 9a.
1980 *Climacograptus angustus* (Perner). – Koren' & Mikhaylova *in* Koren' *et al.*, p. 132, text-fig. 35.
1980 *Climacograptus* aff. *angustus* (Perner). – Koren' & Mikhaylova *in* Koren' *et al.*, p. 131, pl. 37, figs 2–7; text-fig. 34.

Figure 7. A – *Avitograptus* sp. aff. *A. avitus* (Davies, 1929); KD-HB-48-07. • B – *Metabolograptus wangjiawanensis* (Mu & Lin, 1984); XKDE2-28a-1. • C – *Persculptograptus* sp.; KD-HB-48-10. • D, F, H, I – *Paramplexograptus*? sp.; D – DKM2-0.5-2; F – XAS50-xx; H – XKDE2-5-1; I – XKDE2-24. • E, G – *Normalograptus mirnyensis* (Obut & Sobolevskaya, *in* Obut *et al.*, 1967); E – XAS50-57; G – XKT1-13-2. • J – *Metabolograptus parvulus* (Lapworth, 1900); J – XKDE2-42. • K – *Korenograptus jerini* (Koren' & Melchin, 2000); E2-49a-1. All scale bars represent 1 mm.


A
B
C
D
E
F
G
H
I
J
K

1984 *Climacograptus angustus* (Perner). – Chen, p. 38, pl. 2, figs 9, 10; text-fig. 3(j).
p. 1988 *Scalarigraptus angustus* (Perner). – Riva, p. 232, figs 3a–c, j?, k?, t–v?
1993 *Normalograptus angustus* (Perner). – Štorch & Serpagli, p. 22, pl. 1, figs 3, 4, 6?; pl. 2, figs 2, 6; text-fig. 7a?, b, c, f.
2000 *Normalograptus angustus* (Perner). – Koren' & Melchin, p. 1097, figs 4.8, 4.11–4.13, 5.4.
.2007 *Normalograptus angustus* (Perner). – Chen *et al*., pp. 80, 81, text-fig. 3R.
.2011 *Normalograptus angustus* (Perner). – Goldman *et al*., p. 228, fig. 1K [see pre-2015 synonymy of *Normalograptus angustus* in Kraft *et al*. 2015].
2015 *Normalograptus angustus* (Perner). – Kraft *et al*., pp. 215–217, figs 8A, B, 9A–F, 13B, F, G [see for synonymy list].

Material. – Four specimens from the Tierekeawati section.

Description. – The mature rhabdosome measures up to 8.25 mm long. It widens from 0.6–0.8 mm at the first thecal pair to the maximum width of 0.9–1.2 mm distally. 2TRD is 1.4–1.7 mm at $th2^1$, 1.8 mm distally. The thecae are sub-alternating, box-like, and of climacograptid form with sharp, non-hooded genicula. The supragenicular walls are straight and parallel to the rhabdosome axis. The sicula is slender, with a length of 1.2–1.4 mm and a width of 0.25 mm. $Th1^1$ first grows downward and then turns upward just below the sicular aperture. The upward-growing portion of theca 1^1 is 0.6–0.9 mm long. $Th1^2$ crosses the sicula diagonally, leaving the dorsal side of the sicula exposed for *ca* 0.2 mm. The median septum can be observed to originate at the second thecal pair.

Discussion. – Riva (1988) re-studied the type material of both *N. miserabilis* and *N. angustu*s and supported the synonymy of *N. miserabilis* and *N. angustus*, as was first suggested by Příbyl (1949) and later supported by Skoglund (1963), Bjerreskov (1975), Koren' & Mikhaylova (*in* Koren' *et al*. 1980) and Chen (1984). However, *N. miserabilis* was referred to *Styracograptus* by Goldman *et al*. (2011) after they restudied the type material and found that the two taxa have significantly different internal structures and thus should be assigned to different genera. Some of Riva's (1988) specimens of *N. angustus* from Anticosti Island with densely spaced thecae (text-fig. 3d–h) were assigned to *M. parvulus* by Zalasiewicz & Tunnicliff (1994). Other specimens with slightly concave, inclined supra-genicular walls (text-fig. 3t–v) were reassigned to *N.* aff. *N. indivisus* by Chen *et al*. (2005). *Normalograptus angustus* differs from *N. acceptus* (Koren' & Mikhaylova *in* Koren' *et al*., 1980) in not having hooded genicula, and from *N. mirnyensis* (Obut & Sobolevskaya *in* Obut *et al*., 1967) in having a narrower distal width and less closely spaced thecae.

Stratigraphical range. – *Normalograptus angustus* has been recorded from the *Pleurograptus linearis* Biozone (Skoglund 1963), and also from the *M. extraordinarius* and *P. persculptus* biozones in South China (Chen *et al*. 2005). It has also been reported from high in the Rhuddanian, from the *Co. cyphus* Biozone (Rickards 1970, Hutt 1974); is also known from the *A. cuneatus* and *H. sinitzini* subzones (*Ak. ascensus–Pk. acuminatus* Biozone) of the Kurama Range, Eastern Uzbekistan (Koren' & Melchin 2000).

***Normalograptus mirnyensis* (Obut & Sobolevskaya *in* Obut *et al*., 1967)**
Figures 4A, E, G, H, J, L, M, R, X, 7E, G, 8A, C

* 1967 *Hedrograptus mirnyensis* Obut & Sobolevskaya *in* Obut *et al*., p. 47, pl. 1, figs 4–9.
.1984 *Climacograptus mirnyensis* (Obut & Sobolevskaya). – Chen, p. 38, pl. 2, figs 12–14; text-fig. 3f–h.
.1999 *Normalograptus mirnyensis* (Obut & Sobolevskaya). – Li, p. 95, pl. 1, fig. 9.
.1999 *Climacograptus minutus* Carruthers. – Li, p. 89, pl. 1, figs 6, 8, 10, 12; pl. 10, fig. 11.
.2007 *Normalograptus mirnyensis* (Obut & Sobolevskaya). – Loydell, pp. 37–38, text-figs 19A–E [see for synonymy list].
.2007 *Normalograptus mirnyensis* (Obut & Sobolevskaya). – Chen *et al*., text-figs 3C, 4C.
.2011 *Normalograptus mirnyensis* (Obut & Sobolevskaya). – Štorch *et al*., pp. 374–375, figs 25E, F, I, J, 26C, F, K.

Material. – Twenty-four small specimens: twenty from the Tierekeawati section, one from the Sishichang section, and three from the Dawangou section.

Description. – The rhabdosome, which is up to 13 mm long, widens from 0.7–0.8 mm at the first thecal pair to a

Figure 8. A, C – *Normalograptus mirnyensis* (Obut & Sobolevskaya *in* Obut *et al*., 1967); A – XKT1-2b-1; C – XKT1-10-2. • B, E, F – *Metabolograptus parvulus* (Lapworth, 1900); B – XKT1-9; E – DMK2-1.6-36; F – XKT1-55. • D – *Hirsutograptus jideliensis* (Koren' & Mikhaylova *in* Koren' *et al*., 1980); XKT1-10-1. • G, J – *Normalograptus angustus* (Perner, 1895); G – XKT1-28-3; J – XKT1-34. • H – *Normalograptus ajjeri* (Legrand, 1977); XKT1-29. • I – *Paramplexograptus madernii* (Koren' & Mikhaylova *in* Koren' *et al*., 1980); HD-HB-48-21. All scale bars represent 1 mm.


A
B
C
D
E
F
G
H
I
J

maximum width of 0.9–1.1 mm distally. The thecae are of typical climacograptid type, with sharp, non-hooded genicula. The supragenicular walls are straight. Apertural excavations are semi-ovoid in shape. The 2TRD is 1.45 to 1.6 mm at the proximal end, 1.4–1.7 mm distally. The sicula measures 1.20–1.4 mm long. Th1^1 first grows downward and then turns upward just below the sicular aperture. The upward-growing portion of theca 1^1 is 0.8 mm long. The sicula is exposed below th1^2 for 0.3–0.4 mm. There is a full median septum. The interthecal septa are long and straight.

Discussion. – Normalograptus mirnyensis is characterized by its small 2TRD values, parallel-sided supragenicular walls and strong thecal geniculation. It differs from *N. angustus* in having more densely spaced thecae throughout the rhabdosome. *Normalograptus mirnyensis* can be distinguished from *N. ajjeri* by having a narrower rhabdosome and less widely spaced thecae. *Normalograptus mirnyensis* differs from *N. acceptus* in having a slightly wider rhabdosome and less distinct genicular flanges.

The specimens described herein have blunt proximal ends and short virgellae, resembling specimens from north-central Nevada described by Štorch *et al*. (2011) and from Jordan described by Loydell (2007, with long virgellae). Other specimens referred to this species, reported from the Upper Yangtze Region in South China (Chen *et al*. 2005) and from eastern Uzbekistan (Koren' & Melchin 2000), have more tapering proximal ends.

Stratigraphical range. – N. mirnyensis is recorded from the *Ak. ascensus–Pk. acuminatus* Biozone of Mirny Creek, northeast Russia (Obut *et al*. 1967), and from the *N. lubricus*, *A. cuneatus*, and *H. sinitzini* subzones in the Kurama range, eastern Uzbekistan (Koren' & Melchin 2000). It has been recorded from the *M. extraordinarius* and *P. persculptus* biozones in the Yangtze region, China (Chen *et al*. 2005), and from strata assigned to the upper *P. persculptus* Biozone in Mauritania (northwest Africa) by Underwood *et al.* (1998; see Loydell 2007). The species has been reported from the *M. extraordinarius* to *P. persculptus* biozones in north-central Nevada, USA by Štorch *et al*. (2011).

Family *incertae sedis*

Genus *Hirsutograptus* Koren' & Rickards, 1996, emend. Melchin *et al*., 2011

Type species. – Hirsutograptus longispinosus Koren' & Rickards, 1996.

Diagnosis. – Species with Pattern I aseptate rhabdosomes with glyptograptid to climacograptid thecae; nema embedded in the obverse rhabdosomal wall or with a narrow, obverse partial median septum (Melchin *et al*. 2011).

***Hirsutograptus jideliensis* (Koren' & Mikhaylova *in* Koren' *et al*., 1980)**

Figures 3B, G, 5A, E, F, G, M, O, P, 8D

*1980 *Climacograptus jideliensis* Koren' & Mikhaylova *in* Koren' *et al*., pp. 133–134, pl. 37, figs 8–12; text-fig. 36a–d.

.2000 *Climacograptus jideliensis* Koren' & Mikhaylova. – Koren' & Melchin, pp. 1097–1098, text-figs 4.17–4.28, 5.13–5.15, 6.1.

2011 *Hirsutograptus jideliensis* (Koren' & Mikhaylova). – Melchin *et al*., pp. 294, 301.

Material. – Twenty-one specimens: twenty specimens from the Tierekeawati section and one from the Dawangou section.

Description. – Rhabdosome up to 7.8 mm long, widening from 0.6–0.9 mm at the first thecal pair to the maximum width of 0.9–1.2 mm distally. The 2TRD is 1.1–1.5 mm at th2^1, 1.4–1.55 mm distally. Thecae have horizontal apertures and distinct, sharp genicula and narrow genicular flanges. Th1^1 first grows downward and turns upward just below the sicular aperture with an upward-growing portion 0.65–0.9 mm long. Th1^2 crosses the sicula diagonally, leaving the antivirgellar side of the sicula exposed for *ca* 0.2–0.3 mm. There is a full median septum, originating at the second thecal pair.

Discussion. – Hirsutograptus jideliensis is characterized by its rounded proximal end and densely spaced thecae with short genicular flanges. The present specimens are close to those from the type area, but have a slightly narrower maximum rhabdosomal width. Moreover, the present specimens have an earlier origination for the median septum, which starts at the second thecal pair. *Hirsutograptus jideliensis* differs from *N. acceptus* (Koren' & Mikhaylova *in* Koren' *et al*., 1980) in having shorter genicular flanges and wider rhabdosome width.

Stratigraphic range. – Hirsutograptus jideliensis is recorded from the *Pk. acuminatus* Biozone in Kazakhstan (Koren' & Mikhaylova *in* Koren' *et al*. 1980) and from the *N. lubricus*, *A. cuneatus*, and *H. sinitzini* subzones (*Ak. ascensus–Pk. acuminatus* Biozone) in the Kurama Range, Eastern Uzbekistan (Koren' & Melchin 2000).

Acknowledgements

This work was financially supported by the National Natural Science Foundation of China (Nos 41402010 and 41172012). The special foundation of the Key Laboratory of Economic Stratigraphy and Palaeogeography, Nanjing Institute of Geology and Palaeontology (No. Y421140303) is also acknowledged here. Wang Yi, Xu Honghe, Yan Kui, Liang Yan and Zhang Xiaole from NIGPAS (Nanjing, China) are thanked for their great help during fieldwork. This manuscript benefited greatly from reviews by M.J. Melchin and an anonymous reviewer. M.J. Melchin also provided valuable insights into systematic issues surrounding many of the present taxa in an earlier draft of this paper.

References

Anhui Geological Survey Team (ed.) 1982. *Graptolites from Anhui*. 166 pp. Anhui Science and Technology Publishing House, Hefei.

Baarli, B.G. 2014. The early Rhuddanian survival interval in the Lower Silurian of the Oslo Region: a third pulse of the end-Ordovician extinction. *Palaeogeography, Palaeoclimatology, Palaeoecology 395*, 29–41. DOI 10.1016/j.palaeo.2013.12.018

Bengtson, P. 1988. Open nomenclature. *Palaeontology 31(1)*, 223–227.

Bergström, S.M., Saltzman, M.R. & Ausich, W.I. 2003. Conodonts, graptolites, and $\delta^{13}C$ chemostratigraphy in the latest Ordovician (Gamachian, Hirnantian): A global review. *Geological Society of America, Abstracts with Programs 35(2)*, 14.

Berry, W.B.N. 1986. Stratigraphic significance of Glyptograptus persculptus group graptolites in central Nevada, U.S.A., 135–143. *In* Hughes, C.P., Rickards, R.B. & Chapman, A.J. (eds) *Palaeoecology and biostratigraphy of graptolites. Geological Society of London, Special Publication 20*.

Bjerreskov, M. 1975. Llandoverian and Wenlockian graptolites from Bornholm. *Fossils and Strata 8*, 1–94.

Blackett, E., Page, A., Zalasiewicz, J., Williams, M., Rickards, B. & Davis, J. 2008. A refined graptolite biostratigraphy for the Late Ordovician-early Silurian of central Wales. *Lethaia 42*, 83–96. DOI 10.1111/j.1502-3931.2008.00108.x

Bronn, H.G. 1849. *Index Palaeontogicus B, Enumerator Palaeontologicus*. 980 pp. E. Schweizerbart'sche Verlagsbuchhandlung, Stuttgart.

Bulman, O.M.B. 1955. Graptolithina with sections on Enteropneusta and Pterobranchia, 1–101. *In* Moore, R.C. (ed.) *Treatise on invertebrate paleontology*. Geological Society of America & University of Kansas Press, Lawrence & Boulder.

Chen, X. 1984. Silurian graptolites from southern Shaanxi and northern Sichuan with special reference to classification of Monograptidae. P*alaeontologica Sinica, New Series B 20*, 1–102.

Chen, X., Fan, J.X., Melchin, M.J. & Mitchell, C.E. 2005. Hirnantian (latest Ordovician) graptolites from the Upper Yangtze Region, China. *Palaeontology 48*, 235–280. DOI 10.1111/j.1475-4983.2005.00453.x

Chen, X., Ni, Y.N., Mitchell, C.E., Qiao, X.D. & Zhan, S.G. 2000b. Graptolites from the Qilang and Yigan Formations (Caradoc, Ordovician) of Kalpin, Western Tarim, Xinjiang, China. *Journal of Paleontology 74(2)*, 282–300. DOI 10.1666/0022-3360(2000)074<0282:GFTQAY>2.0.CO;2

Chen, X., Rong, J.Y., Fan, J.X., Zhan, R.B., Mitchell, C.E., Harper, D.A.T., Melchin, M.J., Peng, P.A., Finney, S.C. & Wang, X.F. 2006. The Global boundary Stratotype Section and Point (GSSP) for the base of the Hirnantian Stage (the uppermost of the Ordovician System). *Episodes 29(3)*, 183–196.

Chen, X. & Wang, Z.H. 2003. Global auxiliary stratotype section of the Upper Ordovician in China. *Journal of Stratigraphy 27(3)*, 264–265.

Chen, X., Zhan, R.B., Zhang, Y.D., Rong, J.Y., Mitchell, C.E., Harper, D.A.T., Li, R.Y. & Wang, Y. 2000a. Late Ordovician to earliest Silurian graptolite and brachiopod biozonation from the Yangtze region, South China with a global correlation. *Geological Magazine 137*, 623–650. DOI 10.1017/S0016756800004702

Chen, X., Zhang, Y.D. & Li, Y. 1995. Ordovician Basin analysis of China, 245–250. *In* Cooper, J.D., Droser, M.L. & Finney, S.C. (eds) *Ordovician Odyssey: Short Papers for the Seventh International Symposium on the Ordovician System.* SEPM (Pacific Section of the Society of Sedimentary Geology) 77, Fullerton.

Chen, X., Zhang, Y.D., Yu, G.H. & Liu, X. 2007. Latest Ordovician and earliest Silurian graptolites from northwestern Zhejiang, China. *Acta Palaeontologica Sinica 46*, 77–82.

Churkin, M. Jr. & Carter, C. 1970. Early Silurian graptolites from southeastern Alaska and their correlation with graptolitic sequences in North America and the Arctic. *United States Geological Survey, Professional Paper 653*, 1–51.

Cooper, R.A., Sadler, P.M., Munnecke, A. & Crampton, J. 2014. Graptoloid evolutionary rates track Ordovician-Silurian global climate change. *Geological Magazine 151(2)*, 349–364. DOI 10.1017/S0016756813000198

Davies, K.A. 1929. Notes on the graptolite faunas in the Upper Ordovician and Lower Silurian. *Geological Magazine 66*, 1–27. DOI 10.1017/S0016756800099763

Elles, G.L. & Wood, E.M.R. 1906. A monograph of British graptolites. Part 5. *Monograph of the Palaeontographical Society 60(288)*, lxxiii–xcvi + 181–216.

Elles, G.L. & Wood, E.M.R. 1907. A monograph of British graptolites. Part 6. *Monograph of the Palaeontographical Society 61(297)*, xcvii–cxx + 217–272.

Elles, G.L. & Wood, E.M.R. 1908. A monograph of British graptolites. Part 7. *Monograph of the Palaeontographical Society 62(305)*, cxxi–cxlviii + 273–358.

Fan, J.X. & Chen, X. 2007. Preliminary report on the Late Ordovician graptolite extinction in the Yangtze region. *Palaeogeography, Palaeoclimatology, Palaeoecology 245*, 82–94. DOI 10.1016/j.palaeo.2006.02.019

Fan, J.X., Melchin, M.J., Chen, X., Wang, Y., Zhang, Y.D., Chen, Q., Chi, Z.L. & Chen, F. 2011. Biostratigraphy and geography of the Ordovician-Silurian Lungmachi black shales in South China. *Science China Earth Science 54*, 1854–1863. DOI 10.1007/s11430-011-4301-3

Fang, Y.T., Liang, S.J., Zhang, D.L. & Yu, J.L. 1990. *Stratigraphy and graptolite fauna of Lishuwo Formation from Wuning,* *Jiangxi*. 155 pp. Nanjing University Publishing House, Nanjing.

Feng, Z.Z., Bao, Z.D., Wu, M.B., Jin, Z.K., Shi, X.Z. & Luo, A.R. 2007. Lithofacies palaeogeography of the Ordovician in Tarim area. *Journal of Palaeogeography 9(5)*, 447–460.

Frech, F. 1897. *Lethaea Geognostica. Lethaea Paleozoica 1, 11. Graptolithen*, 544–684. E. Schweizerbart'sche Verlagsbuchhandlung, Stuttgart.

Fortey, R.A. & Cocks, L.R.M. 2003. Palaeontological evidence bearing on global Ordovician-Silurian continental reconstructions. *Earth-Science Reviews 61(3/4)*, 245–307. DOI 10.1016/S0012-8252(02)00115-0

Fu, H.Y. 1982. Graptolithina, 410–479. *In* Geological Bureau of Hunan (ed.) *The palaeontological atlas of Hunan*. Geological Publishing House, Beijing.

Goldman, D., Mitchell, E.C., Melchin, J.M., Fan, J.X., Wu, S.Y. & Sheet, H.D. 2011. Biogeography and mass extinction: extirpation and re-invasion of *Normalograptus* species (Graptolithina) in the Late Ordovician palaeotropics. *Proceedings of the Yorkshire Geological Society 58(4)*, 227–246. DOI 10.1144/pygs.58.4.300

Harper, D.A.T., Hammarlund, E.U. & Rasmussen, C.M. 2013. End Ordovician extinctions: a coincidence of causes. *Gondwana Research 25(4)*, 1294–1307. DOI 10.1016/j.gr.2012.12.021

Hsü, S.C. 1934. The graptolites of the Lower Yangtze Valley. *Bulletin of the National Research Institute of Geology, Academia Sinica, Series A 4*, 1–106.

Hutt, J.E. 1974. The Llandovery graptolites of the English Lake District. Part 1. *Monograph of the Palaeontographical Society 128(540)*, 1–56.

Jiang, D.Y., Hao, W.C., Bai, S.L., Wang, X.P. & Yao, J.X. 2001. New progress of the study on Late Ordovician-Early Carboniferous stratigraphic division and correlation in Tarim Basin, Xinjiang. *Acta Scientiarum Naturalium Universitatis Pekinensis 37(4)*, 529–536.

Jiang, D.Y., Pi, X.J., Sun, Z.Y., Chen, Y., Wu, F.X. & Hao, W.C. 2006. Report on graptolite biostratigraphy of the basal part of the Middle Member of the Kepingtage Formation at Dawangou section, Keping, Xinjiang. *Journal of Stratigraphy 30(3)*, 253–257.

Koren', T.N., Ahlberg, P. & Nielsen, A.T. 2003. The post-persculptus and pre-ascensus graptolite fauna in Scania, south-western Sweden: Ordovician or Silurian?, 133–138. *In* Ortega, G. & Aceñolaza, G.F. (eds) *Proceedings, 7th International Graptolite Conference & Field Meeting, Subcommission on Silurian Stratigraphy. INSUGEO, Serie Correlación Geológica 18*.

Koren', T.N. & Melchin, M.J. 2000. Lowermost Silurian graptolites from the Kurama Range, eastern Uzbekistan. *Journal of Paleontology 74*, 1093–1113. DOI 10.1666/0022-3360(2000)074<1093:LSGFTK>2.0.CO;2

Koren', T.N., Mikhaylova, N.F. & Tsai, D.T. 1980. Graptolity, 121–170. *In* Apollonov, M.K., Bandaletov, S.M. & Nikitin, J.F. (eds) *Granitsa ordovika i silura v Kazakhstane*. Nauka Kazakh SSR Publishing House, Alma-Ata.

Koren', T.N. & Rickards, R.B. 1996. Taxonomy and evolution of graptoloids from the southern Urals, western Kazakhstan. *Special Papers in Palaeontology 54*, 1–32.

Koren', T.N. & Rickards, R.B. 2004. An unusually diverse Llandovery (Silurian) diplograptid fauna from the southern Urals of Russia and its evolutionary significance. *Palaeontology 47*, 859–918. DOI 10.1111/j.0031-0239.2004.00411.x

Kraft, P., Štorch, P. & Mitchell, C.E. 2015. Graptolites of the Králův Dvůr Formation (mid Katian to earliest Hirnantian, Czech Republic). *Bulletin of Geosciences 90(1)*, 195–225. DOI 10.3140/bull.geosci.1435

Lankester, E.R. 1877. Notes on the embryology and classification of the animal kingdom: comprising a revision of speculations relative to the origin and significance of the germ-layers. *Quarterly Journal of Microscopical Science, New Series 17*, 399–454.

Lapworth, C. 1873. On an improved classification of the *Rhabdophora*, Part I. *Geological Magazine 10*, 500–504. DOI 10.1017/S0016756800469256

Lapworth, C. 1875. Section Graptoloidea, 631–672. *In* Hopkinson, J. & Lapworth, C. (eds) *Descriptions of the graptolites of the Arenig and Llandeilo rocks of St. Davids. Quarterly Journal of the Geological Society of London 31*.

Lapworth, C. 1876. On Scottish Monograptidae. *Geological Magazine 13*, 350–360, 499–507, 544–552. DOI 10.1017/S0016756800154998

Lapworth, C. 1877. On the graptolites from County Down. *Proceedings of the Belfast Naturalists' Field Club (Appendix) 1876/ 77*, 125–144.

Lapworth, H. 1900. The Silurian sequence of Rhayader. *Quarterly Journal of the Geological Society of London 56*, 67–137. DOI 10.1144/GSL.JGS.1900.056.01-04.09

Legrand, P. 1977. Contribution à l'étude des graptolites du Llandoverien inférieur de L'Oued in Djerane (Tassili N'Ajjer oriental, Sahara algérien). *Bulletin de la Société d'Histoire Naturelle de l'Afrique du Nord 67*, 141–196.

Legrand, P. 1987. Modo de desarrollo del suborden Diplograptina (Graptolithina) en el Ordovicico Superior y en el Silurico. *Revista Española de Paleontología 2*, 59–64.

Li, J.J. 1984. Graptolites across the Ordovician-Silurian boundary from Jingxian, Anhui, 309–370. *In* Nanjing Institute of Geology and Palaeontology, Academia Sinica (ed.) *Stratigraphy and palaeontology of systemic boundaries in China, Ordovician-Silurian boundary 1*. Anhui Science and Technology Publishing House, Hefei.

Li, J.J. 1995. Lower Silurian graptolites from the Yangtze Gorge district. *Palaeontologica Cathayana 6*, 215–344.

Li, J.J. 1999. Lower Silurian graptolites from southern Anhui. *Bulletin of the Nanjing Institute of Geology and Palaeontology, Academia Sinica 14*, 70–157.

Lin, Y.K. & Chen, X. 1984. Glyptograptus persculptus Zone–the earliest Silurian graptolite zone from Yangzi Gorges, China, 203–232. *In* Nanjing Institute of Geology and Palaeontology, Academia Sinica (ed.) *Stratigraphy and palaeontology of systemic boundaries in China, Ordovician-Silurian boundary 1*. Anhui Science and Technology Publishing House, Hefei.

Loydell, D.K. 2007. Graptolites from the Upper Ordovician and

Lower Silurian of Jordan. *Special Papers in Palaeontology 78*, 1–66.

Loydell, D.K., Mallett, A.M., Mikulic, D.G., Kluessendorf, J. & Norby, R.D. 2002. Graptolites from near the Ordovician-Silurian boundary in Illinois and Iowa. *Journal of Paleontology 76*, 134–137. DOI 10.1666/0022-3360(2002)076<0134:GFNTOS>2.0.CO;2

Maletz, J. 2014. The classification of the Pterobranchia (Cephalodiscida and Graptolithina). *Bulletin of Geosciences 89(3)*, 477–540. DOI 10.3140/bull.geosci.1465

Maletz, J., Ahlberg, P., Suyarkova, A. & Loydell, D.K. 2014. Silurian graptolite biostratigraphy of the Röstånga-1 drill core, Scania – a standard for southern Scandinavia. *GFF 136(1)*, 175–178. DOI 10.1080/11035897.2013.865665

Matthews, S.C. 1973. Notes on open nomenclature and synonymy lists. *Palaeontology 16*, 713–719.

Melchin, M.J. 1998. Morphology and phylogeny of some early Silurian 'diplograptid' genera from Cornwallis Island, Arctic Canada. *Palaeontology 41*, 263–315.

Melchin, M.J. 2008. Restudy of some Ordovician–Silurian boundary graptolites from Anticosti Island, Canada, and their biostratigraphic significance. *Lethaia 41*, 155–162. DOI 10.1111/j.1502-3931.2007.00045.x

Melchin, M.J. & Holmden, C. 2006. Carbon isotope chemostratigraphy in Arctic Canada: sea-level forcing of carbonate platform weathering and implications for Hirnantian global correlation. *Palaeogeography, Palaeoclimatology, Palaeoecology 234*, 186–200. DOI 10.1016/j.palaeo.2005.10.009

Melchin, M.J., McCracken, A.D. & Oliff, F.J. 1991. The Ordovician-Silurian boundary on Cornwallis and Truro islands, Arctic Canada: preliminary data. *Canadian Journal of Earth Sciences 28*, 1854–1862. DOI 10.1139/e91-165

Melchin, M.J. & Mitchell, C.E. 1991. Late Ordovician extinction in the Graptoloidea, 143–156. *In* Barnes, C.R. & Williams, S.H. (eds) *Advances in Ordovician geology. Geological Survey of Canada, Paper 90-9*.

Melchin, M.J., Mitchell, C.E., Naczk-Cameron, A., Fan, J.X. & Loxton, J. 2011. Phylogeny and adaptive radiation of the Neograptina (Graptoloida) during the Hirnantian mass extinction and Silurian recovery. *Proceedings of the Yorkshire Geological Society 58*, 281–309. DOI 10.1144/pygs.58.4.301

Melott, A.L. & Thomas, B.C. 2009. Late Ordovician geographic patterns of extinction compared with simulations of astrophysical ionizing radiation damage. *Paleobiology 35(3)*, 311–320. DOI 10.1666/0094-8373-35.3.311

Mitchell, C.E. 1987. Evolution and phylogenetic classification of the Diplograptacea. *Palaeontology 30*, 353–405.

Mitchell, C.E., Melchin, M.J., Cameron, C.B. & Maletz, J. 2013. Phylogenetic analysis reveals that *Rhabdopleura* is an extant graptolite. *Lethaia 46*, 34–56. DOI 10.1111/j.1502-3931.2012.00319.x

Mu, E.Z., Li, J.J. & Ge, M.Y. 1960. Ordovician graptolites from Xinjiang (Sinkiang). *Acta Palaeontologica Sinica 8*, 27–39. [in Chinese with English summary]

Mu, E.Z. & Ni, Y.N. 1983. Uppermost Ordovician and lowermost Silurian graptolites from the Xainza area of Xizang (Tibet) with discussion on the Ordovician-Silurian boundary. *Palaeontologia Cathayana 1*, 151–179.

Mu, E.Z. & Lin, Y.K. 1984. Graptolites from the Ordovician-Silurian boundary sections of Yichang area, W. Hubei, 45–82. *In* Nanjing Institute of Geology and Palaeontology, Academia Sinica (ed.) *Stratigraphy and palaeontology of systemic boundaries in China, Ordovician-Silurian boundary 1*. Anhui Science and Technology Publishing House, Hefei.

Nanjing Institute of Geology and Mineral Resources (ed.) 1983. *Palaeontological atlas of east China, 1. Early Paleozoic*. 657 pp. Geological Publishing House, Beijing.

Ni, Y.N. & Chen, X. 1997. Graptolites from bore cores of Northern Tarim Basin, Xinjiang. *Acta Palaeontologica Sinica 36 (sup.)*, 155–167.

Nicholson, H.A. 1868. On the graptolites of the Coniston Flags; with notes on the British species of the genus *Graptolites*. *Quarterly Journal of the Geological Society of London 24*, 521–545. DOI 10.1144/GSL.JGS.1868.024.01-02.67

Nicholson, H.A. 1869. On some new species of graptolites. *Annals and Magazine of Natural History 4*, 231–242. DOI 10.1080/00222936908696041

Obut, A.M. 1955. Graptolity, 136–139. *In* Nikiforova, O.I. (ed.) *Polevoy atlas ordovikskoy i silurskoy fauny Sibirskoy platformy*. Gosgeoltechizdat, Moskva. [in Russian]

Obut, A.M. & Sennikov, N.V. 1985. Osobennosti llandoveriyskikh planktonovykh soobschestv Sibirskoy platformy, 51–60. *In* Betechtuna, O.A. & Zhuravleva, I.T. (eds) *Sreda i zhizn v geologicheskom proshlom (Paleobasseiny i ich obitateli). Trudy Instituta geologii i geofiziki 628*. Nauka, Novosibirsk. [in Russian]

Obut, A.M., Sobolevskaya, R.F. & Nikolaev, A.N. 1967. *Graptolites and stratigraphy of Lower Silurian parts of the uplifted Kolyma Massif.* 162 pp. Nauka, Moskva.

Packham, G.H. 1962. Some diplograptids from the British Lower Silurian. *Palaeontology 5*, 498–526.

Perner, J. 1895. *Studie o českých graptolitech II*. 52 pp. Česká akademie císaře Františka Josefa pro vědy, slovesnost a umění, Praha.

Přibyl, A. 1949. Revision of the Diplograptidae and Glossograptidae of the Ordovician of Bohemia. *Bulletin Internationale de l'Académie Tchèque des Sciences 50*, 1–51.

Rickards, R.B. 1970. The Llandovery (Silurian) graptolites of the Howgill Fells, northern England. *Monograph of the Palaeontographical Society 123(524)*, 1–108.

Riva, J. 1988. Graptolites at and below the Ordovician-Silurian boundary on Anticosti Island, Canada, 221–237. *In* Cocks, L.R.M. & Rickards, R.B. (eds) *A global analysis of the Ordovician-Silurian Boundary. Bulletin of the British Museum (Natural History) Geology 43*, 1–394.

Skoglund, R. 1963. Uppermost Viruan and lower Harjuan (Ordovician) stratigraphy of Västergötland and lower Harjuan graptolite faunas of central Sweden. *Bulletin of the Geological Institutions of the University of Uppsala 42*, 1–55.

Štorch, P. & Feist, R. 2008. Lowermost Silurian graptolites of Montagne Noire, France. *Journal of Paleontology 82(5)*, 938–956. DOI 10.1666/07-004.1

Štorch, P., Mitchell, C.E., Finney, S.C. & Melchin, M.J. 2011. Uppermost Ordovician (upper Katian–Hirnantian) graptolites of north-central Nevada, U.S.A. *Bulletin of Geosciences 86(2)*, 301–386. DOI 10.3140/bull.geosci.1264

Štorch, P. & Serpagli, E. 1993. Lower Silurian graptolites from southwestern Sardinia. *Bollettino della Società Paleontologica Italica 32*, 3–57.

Štorch, P. & Schönlaub, H.P. 2012. Ordovician-Silurian boundary graptolites of the Southern Alps, Austria. *Bulletin of Geosciences 87(4)*, 755–766. DOI 10.3140/bull.geosci.1350

Underwood, C.J., Deynoux, M. & Ghienne, J.-F. 1998. High palaeolatitude (Hodh, Mauritania) recovery of graptolite faunas after the Hirnantian (end Ordovician) extinction event. *Palaeogeography, Palaeoclimatology, Palaeoecology 142*, 91–105. DOI 10.1016/S0031-0182(98)00070-4

Wang, H.H., Li, J.H., Yang, J.Y., Zhou, X.B., Fu, C.J. & Li, W.S. 2013. Paleoplate reconstruction and drift path of Tarim block from Neoproterozic to early Palaeozoic. *Advances in Earth Science 28(6)*, 637–647.

Wang, Y. 2010. The sporomorphs from the Late Ordovician to Early Silurian in China and their palaeogeographical implication. *Acta Palaeontologica Sinica 49(1)*, 1–9.

Waern, B. 1948. The Silurian strata of the Kullatorp Core. *Bulletin of Geological Institute of Uppsala 32*, 433–474.

Williams, S.H. 1983. The Ordovician-Silurian boundary graptolite fauna of Dob's Linn, southern Scotland. *Palaeontology 26*, 605–630.

Zalasiewicz, J. & Tunnicliff, S. 1994. Uppermost Ordovician to Lower Silurian graptolite biostratigraphy of the Wye Valley, central Wales. *Palaeontology 37*, 695–720.

Zhao, W.J., Wang, S.T., Wang, J.Q. & Zhu, M. 2009. The subdivision and correlation of the Silurian fish-bearing strata and Caledonian movement in Kalpin and Bachu regions, the Tarim Basin, Xinjiang. *Journal of Stratigraphy 33(3)*, 225–240.

Zhan, S.G. 1996. Graptolite-bearing strata of the Well YM-2 in Tarim Basin. *Journal of Xinjiang Petroleum Institute 8(1)*, 1–5.

Zhan, S.G. 1997. Graptolite-bearing strata of Well Qk-1 and Well C-1 in Tarim Basin. *Journal of Xinjiang Petroleum Institute 9(1)*, 1–6.

Zhou, Z.Y. 2001. *Stratigraphy of the Tarim Basin*. 335 pp. Science Press, Beijing.

Zhou, Z.Y., Chen, X., Wang, Z.H., Wang, Z.Z., Li, J., Geng, L.Y., Fang, Z.J., Qiao, X.D. & Zhang, T.Y. 1991. Ordovician, 56–130. *In* Zhou, Z.Y. & Chen, P.J. (eds) *Biostratigraphy and geological evolution of Tarim*. Science Press, Beijing.